Shear strength estimation of a FRP-strengthened RC beam: A comparison between an artificial neural network and guideline equations

Hamid Nezaminia [iD]

Department of Civil Engineering, Faculty of Engineering, University of Kashan, Kashan, Iran.

Abstract

In recent years, several experimental tests have been conducted on the shear strengthening of reinforced concrete (RC) beams strengthened by fiber-reinforced polymer (FRP) systems. In this regard, some equations have also been proposed to estimate the shear strength of beams reinforced with FRP systems. The aim of this study is to investigate the estimation of the shear strength of beams reinforced with FRP systems using an artificial neural network model. For this purpose, a comprehensive and extensive review of forty published articles has been carried out to compile data on 304 RC beams strengthened with externally bonded FRP systems to improve their shear strength. These laboratory results have been used to provide a database for the ANN model to evaluate the shear behavior. The input to the ANN model consists of the 11 variables, including the sectional geometry, reinforcement ratio, FRP ratio, and the characteristics of concrete, steel reinforcement, and composite material, while the output variable is the shear strength of the FRP-strengthened RC beam. In order to evaluate the effectiveness of the neural network model in estimating the shear capacity of RC beams, the results obtained from the neural network model are compared with the equations from the Publication No. 345 and ACI 440.2R guidelines. The comparison of the results shows that the predictive power of the proposed model is much better than the experimental guidelines. Specifically, the mean absolute relative error (MARE) criteria for the studied data is 13%, 34% and 39% for the ANN model, ACI 440.2R guideline and the Publication No. 345 guideline, respectively.

Keywords: concrete beam, fiber-reinforced polymers, shear strength, artificial neural network, ACI440.2R

1. Introduction

All over the world, concrete bridges and structures require reconstruction, repair, strengthening or complete replacement as they approach the end of the structure's service life, increase in traffic loads, change of use and reduced structural integrity caused by corrosion to the reinforcing steel (Mabsout et al., 2004; Noël & Soudki, 2011; Saadatmanesh & Ehsani, 1991). The use of polymer-based composites for the improvement of reinforced concrete structures has grown significantly in recent years. Fiber-reinforced polymers are among the most desirable materials for repair due to their high strength-to-weight ratio and anti-corrosion properties and can lead to an increase in the service life of the structure (Saadatmanesh & Ehsani, 1991; Shahawy et al., 1996; Sobuz et al., 2011). In general, the strengthening of existing concrete structures or their restoration due to the lack of proper design and construction, lack of maintenance and repair, structural events such as earthquakes, bearing double design loads, improving deficiencies caused by erosion, increasing the structure's

ductility, or other cases by using suitable materials, and the correct implementation methods are done conventionally (Gamino et al., 2010; Sobuz et al., 2011). The use of composite materials made of fibers embedded in a polymer resin medium as polymers reinforced with FRP fibers has been introduced as a necessity in replacing traditional materials and existing practices (Beber & Campos-Filho, 2005). An FRP system is defined as the fibers and resins used to create the composite laminate, all applicable resins used to bond it to the concrete substrate, and all applied coatings used to protect the constituent materials. Coatings used exclusively for aesthetic reasons are not considered part of an FRP system. FRP materials are lightweight, noncorrosive, and exhibit high tensile strength. These materials are readily available in several forms, ranging from factory-made laminates to dry fiber sheets that can be wrapped to conform to the geometry of a structure before adding the polymer resin (American Concrete Institute, 2008).

Following the expansion of the need and attention to strengthening using composite materials and in order to apply technical knowledge, design methods have also been developed. Explaining the analysis methods and considering the safety coefficients in the design with economic considerations led to the formulation of the calculation and implementation guidelines and regulations, including the American Concrete Institute (2008) 440.2R regulations, Management and Planning Organization of Iran (MPO) (2006) Publication No. 345, International Federation for Structural Concrete (fib) (2001), National Cooperative Highway Research Program (NCHRP) Report 514 (Mirmiran et al., 2004), and standard Japan Society of Civil Engineers (Maruyama, 2001) pointed out. The International Federation for Structural Concrete (2001) recently published a publication on the guidelines for designing externally bonded FRP reinforcement for RC structures. The CSA-S806 by the Canadian Standard Association (CSA) (2002) is also active in developing and formulating guidelines for FRP systems. In the United States, ACI Guide 440.2R has been published as a guide for the design and implementation of strengthening concrete buildings with FRP systems.

The design equations presented in the guidelines are based on research results on conventional dimensions and proportional prismatic members, while FRP systems have effective performance on other non-prismatic members as well. These guidelines only apply to FRP strengthening systems used as additional tensile reinforcement. It is not recommended to use these systems as compressive reinforcement. While FRP materials can support compressive stresses, there are numerous issues surrounding the use of FRP for compression.

For example, the microbuckling of fibers can occur if any resin voids are present in the laminate; laminates themselves can buckle if not properly adhered or anchored to the substrate, and highly unreliable compressive strengths result from misaligning fibers in the field. Therefore, the compressive strength of FRP materials is ignored (American Concrete Institute, 2008).

The cause of shear failure, even for simple reinforced concrete elements, is a complex mechanism, and this will take a more complicated form with the use of polymer fibers in reinforced concrete elements (Täljsten, 2003). Therefore, estimating the final shear strength of reinforced concrete beams is very important, especially in design cases. In most of the existing design models, the evaluation of the design shear strength of a reinforced concrete beam reinforced with polymer fibers is obtained from the sum of the contributions of concrete, reinforcing steel (stirrups, ties, or spirals), and polymer fibers (Khalifa & Nanni, 2000; Triantafillou & Antonopoulos, 2000). The contribution of the first two cases can be calculated according to the provisions of the existing design regulations. Therefore, the main difference between the existing design patterns lies in how to evaluate the contribution of polymer fibers. In this regard, experimental relationships (Chaallal et al., 1988; Khalifa et al., 1999; Norris et al., 1997; Täljsten, 2003; Triantafillou & Antonopoulos, 2000; Triantafillou & Plevris, 1992; Zhang et al., 2004) and several analytical equations (Chaallal et al., 1988; Ianniruberto & Imbimbo, 2004; Pellegrino & Modena, 2008; Täljsten, 2003) have been introduced using regression analysis of laboratory data. To develop such models, it is necessary to assume a combination and a template for empirical relationships and then obtain unknown parameters. Several studies have been done on beams from different viewpoints (Alambeigi et al., 2020; Areias et al., 2019; Firouzi & Kazemi, 2023; Dadgar-Rad & Firouzi, 2021; Karami et al., 2020; Żur et al., 2023). The success of such a process in the mentioned studies is difficult due to the large number of parameters affecting the strength of the beam.

In contrast, the use of artificial neural networks provides an alternative method that overcomes these problems. An artificial neural network consists of a network of simple processing elements (neurons), which can display the overall complex behavior determined by the relationship between processing elements and system parameters. This unique feature enables the neural network to solve complex problems that cannot be solved with existing analytical methods. This is true even for problems whose mathematical and physical models are not well known. For this reason, the neural network can be used to estimate and

evaluate the shear strength of beams reinforced with appropriate polymer fibers.

The purpose of this study is to investigate the possibility of using a multi-layer feed-forward network to estimate the ultimate shear strength of concrete beams reinforced with polymer fibers. For this purpose, a database has been compiled from the report analyzing the results of the existing articles. Then, in order to evaluate the efficiency and performance of the neural network model in estimating the shear capacity of reinforced beams, the results obtained from the neural network model are compared with the relationship values of regulations from Iran and America.

2. Materials and methods

2.1. FRP materials

The FRP reinforcement system is one of the composite materials consisting of two parts of fiber or reinforcement fibers surrounded by a polymer resin matrix, as shown in Figure 1 (American Concrete Institute, 1996). FRP fibers, which have elastic technical characteristics and are very resistant, are considered the main bearing component in the FRP material (they make up between 40% and 70% of the volume). The FRP resin also basically acts as an adhesive medium that holds the fibers together (Norris et al., 1997). Among the most common resins, e.g., epoxies, polyesters, are often used in a wide range of environmental conditions. The most widely used resins are epoxy resins, which are used to impregnate dry FRP sheets and bond them to reinforced concrete members. The main role of the resin matrix is to transfer shear from the reinforcing fiber to the adjacent material, protect the fiber in environmental conditions, prevent mechanical damage to the fibers, and finally control the local buckling of the fibers under pressure (Shahawy et al., 1996).
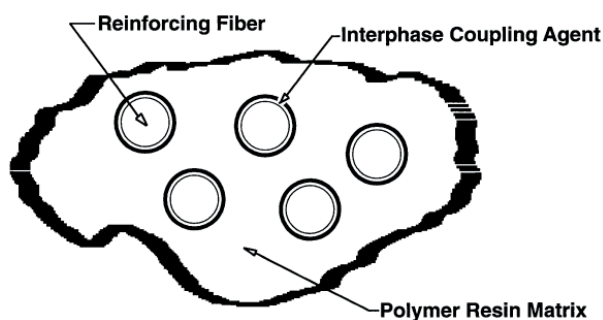

Fig. 1. Components of the FRP system
(American Concrete Institute, 1996)

FRP composite fibers (FRP Sheets) are sheets of FRP with a thickness of several millimeters. FRP sheets are attached to the concrete surface with strong and suitable adhesives. The fibers form the stiffness and strength of the FRP system. In general, 4 types of woven FRP fibers are used for strengthening with FRP, which include carbon fibers, glass, aramid and basalt (International Federation for Structural Concrete, 2001). In FRP reinforcements, one should not rely on their strength to compressive loads. However, their tolerance against the pressure caused by the application of alternating bending anchors or changes in the way of loading can be considered. However, in any case, the compressive strength of FRP reinforcing components is ignored (American Concrete Institute, 2008). Design recommendations are based on limit state design principles. Reinforced or improved concrete buildings with FRP materials are designed based on the recommendations for resistance and serviceability, and from the load factors provided in the Iranian concrete regulations and ACI318 and ACI 440 regulations for American calculations. Additional reduction factors applied to the contribution of the FRP reinforcement are recommended to reflect uncertainties inherent in FRP systems compared with steel reinforced and prestressed concrete. The reduction factors associated with FRP are adjusted to achieve a confidence index above 3.5. Reliability indexes between 3.0 and 3.5 can be encountered in cases where relatively low ratios of steel reinforcement combined with high ratios of FRP reinforcement are used (American Concrete Institute, 2008).

The existing concrete substrate strength is an important parameter for bond-critical applications, including flexure or shear strengthening. It should possess the necessary strength to develop the design stresses of the FRP system through bond. The working concrete, including all repaired surfaces, as well as the main concrete, must have sufficient direct tensile and shear strength to transfer force to the FRP system. The minimum tensile strength of concrete is 1.4 MPa, which is measured by tensile testing according to ACI 503R or ASTM D4541. FRP systems should not be used when the concrete substrate has a compressive strength of less than 17 MPa (American Concrete Institute, 2008; Mirmiran et al., 2004).

When increasing flexure capacity, the structure will be loaded closer to its maximum shear capacity. Täljsten (2003), even shows in a full-scale test that flexural strengthening can induce shear failure. On the other hand, a structure with brittle failure in shear can be strengthened so that the failure mode will change to a more ductile and friendly mode (Carolin & Täljsten, 2005; Collins & Roper, 1990). A beam must have a certain safety margin against shear failure since shear failure is more dangerous

and less predictable than flexural failure (Al-Sulaimani et al., 1994; Carolin & Täljsten, 2005).

There are several methods for shear strengthening, such as additional reinforcements covered with concrete and bracing with steel and CFRP external bonding. For optimal use of the capacity of FRP materials during the shear strengthening of reinforced concrete members by FRP, external reinforcements are attached in the main direction of the fibers, parallel to the maximum of the main tensile stresses. FRPs used for shear reinforcement and repair can be used in three configurations: Complete wrapping, U-Wrap, and bonding to two opposite sides of the beam. In all wrapping schemes, the FRP system can be installed continuously along the span of a member or placed as intermittent (discrete) strips. For the complete wrapping repair technique, the FRP sheet fully wraps the beam cross-section with the fibers fixed in the transverse direction along the beam, as shown in Figure 2 (Chen & Teng, 2003). When the beam is completely wrapped (the most effective case), the probability of debonding is slim, and the full capacity of the FRP sheet can be utilized (American Concrete Institute, 2008). In the U-Wrapping repair technique, the FRP sheet is applied to three sides of the beam's cross-section because the top face is not accessible. For side bonding, the FRP sheets are applied on the two side faces of the beam when the bottom face of the beam is not accessible.
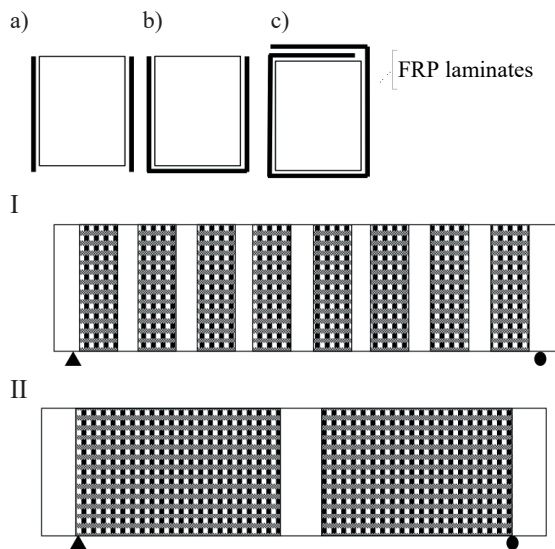
Fig. 2. Schematics of shear reinforcement by adding externally bonded FRP laminates: a) side bonding; b) U-Wrap; c) complete wrapping. Each applied as intermittent strips (I) or a continuous sheet (II) along the length of the member (Chen & Teng, 2003)

FRP debonding is the process where an FRP sheet peels off the concrete surface to which it is bonded. Both ends of the FRP sheet tend to separate from the concrete surface before the FRP sheet reaches its ultimate tensile capacity (Chen & Teng, 2003).

A rupture of an FRP occurs when the materials have reached their ultimate tensile strength, causing the fibers to fracture.

2.2. Neural Network

The most important application of Artificial Neural Networks (ANN) in civil engineering is the estimation of nonlinear functions with appropriate accuracy.

The most common type of neural networks is multi-layer Feed-Forward networks, which consist of an input layer, one or more hidden layers, and an output layer. A weight is considered for each connection. The input layer receives the input data and transmits it to the neurons of the hidden layer. Then, after processing, the data is entered into the output layer. The output of the neurons of the output layer of the prediction neural network is a function of the input data.

There is no universally accepted method for determining the optimal number of neurons and layers for each problem, and for that, it is necessary to act based on experience and trial and error. An example of a feed-forward multilayer neural network is shown in Figure 3.
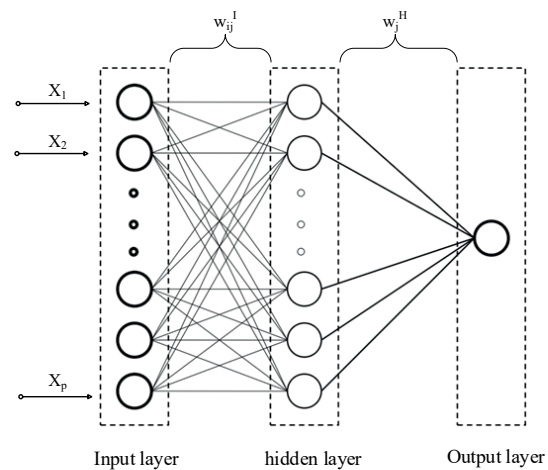
Fig. 3. Schematic diagram of 3-layer network

According to Figure 3, the output in the last layer is obtained from Equation (1):

$$O = f\left(\sum_q g\left(\sum_p x_i w_{ij}^I \right) w_j^H \right) \qquad (1)$$

In this case, I and H represent the input and the hidden layer, respectively, and w represents the

weights of the layers. p and q are the number of input and hidden layer neurons respectively, f is the transfer function of the output layer, and g is the transfer function of the hidden layer. The error backpropagation algorithm is one of the most widely used algorithms for training multi-layer feed-forward artificial neural networks. In this method, the technique of gradient descent is used to minimize the error function, during which the errors are propagated backward from the output layer to the input layer and the weights are modified to minimize the error. Therefore, the training process includes the gradual modification of the weights in order to minimize the error function. This process continues until one of the stopping criteria is satisfied.

Before starting the simulation, the input data should be divided into three groups (Kasabov, 1996):

1. Training data: These data are used among the labeled data to guide the training process, and these data are also used to update the weights of the neural network during training. Typically, 60% to 70% of the total data are randomly selected as training data. After the network has been trained by these data, the weights have found their final value so that the network obtains the least error for the training data.

2. Validation data: This is used to monitor the quality of the neural network model of the system during the learning process and to determine the learning stop condition for the training process (20% of the total data).

3. Test data: after the network was trained by the training data until reaching the minimum error, the rest of the data (remaining 20%) that did not play a role in training was given as input to the network and the network's response with the desired response (their label) is compared and thus the efficiency of the trained network is tested.

3. Methodologies for estimating the shear strength of FRP-strengthened RC beams

Today, due to the increase in the use of FRP materials, numerous regulations and recommendations such as ACI Committee 440.2R (American Concrete Institute, 2008), Management and Planning Organization of Iran (MPO) (2006), International Federation for Structural Concrete (fib) (2001), National Cooperative Highway Research Program (Mirmiran et al., 2004), Japan Society of Civil Engineers (Maruyama, 2001), and Canadian Standard Association (CSA) (2002) have been pub-

lished in different countries of the world for the design of concrete structures reinforced or reinforced with polymer fibers. It seems that flexural reinforcement is well documented in these regulations, although some unclear points remain. This is despite the fact that the behavioral understanding of reinforced concrete structures that are designed for shear strengthening is still at a stage where similar design rules either do not exist or have been addressed briefly (Adhikary & Mutsuyoshi, 2004; Diagana et al., 2003; Pellegrino & Modena, 2002; Täljsten, 2003; Triantafillou & Antonopoulos, 2000). For example, Carolin & Taljsten (2005) have shown that the composite is not uniformly stressed when bonded to the sides of a beam and that the strain field must be studied further to understand the behavior of a member strengthened in shear.

According to Figure 2, the use of externally bonded FRP laminates in typical wrapping schemes (Completely wrapped, U-wraps or side bonding of the web) and the placement of its fibers along the cross-section or perpendicular to the possible shear cracks, effectively increases the shear strength of the elements. The additional shear strength created by this method depends on various parameters such as: sectional geometry, the strengthening pattern, the compressive strength of the concrete, etc. (Diagana et al., 2003; Pellegrino & Modena, 2002; Ozden et al., 2014). Therefore, the amount of this increase in strength is always limited depending on the operation criteria and in accordance with the load conditions of the member. In recent years, several guidelines and design recommendations have been proposed to estimate the shear strength of reinforced concrete beams when they are reinforced with polymer fibers. In all the proposed designs, the design shear strength, V_d, of a concrete beam reinforced with polymer fibers is calculated from Equation (2):

$$V_d = V_c + V_s + V_f \tag{2}$$

where V_c is the contribution of concrete, V_s is the contribution of transverse steel and V_f is the contribution of FRP in the shear strength of the beam. In this regard, V_c and V_s can be obtained by using the relations of the existing regulations, so the main difference between the proposed plans is the way to calculate V_f. In the following, each of these parameters will be explained in the ACI Committee 440.2R (American Concrete Institute, 2008) and the Publication No. 345 (Management and Planning Organization of Iran, 2006). In addition, the method of simulating the shear behavior of reinforced concrete beams reinforced with polymer fibers is explained with the help of a neural network.

3.1. Shear strength of FRP-strengthened RC beams – ACI 440.2R

According to chapter 11 of this regulation, the shear strengthening of members is important because the increase in shear strength leads to flexural failure of the member, which in this case, has a more ductile behavior than shear failure. This regulation stipulates that the design shear strength of concrete member reinforced with FRP system, ($\varnothing V_n$), should be higher than the required shear strength (factored shear), (V_u), in the section under consideration. The design shear strength is calculated by multiplying the nominal shear strength (V_n) by the strength reduction factor according to Equation (3):

$$\varnothing V_n \geq V_u \tag{3}$$

According to American concrete regulations, the strength reduction factor $\varnothing$ is considered equal to 0.85 in shear or torsion mode. The nominal shear strength of a concrete member reinforced with the FRP system is obtained from the total contribution of concrete, shear steel and polymer fibers. Also, an additional reduction factor (Ψ_f) is applied to the contribution of FRP, which is in accordance with Equation (4):

$$V_n = \varnothing(V_c + V_s + \Psi_f V_f) \tag{4}$$

where Ψ_f is equal to 0.95 for the case where the polymer fibers have completely wrapped members, and 0.85 for the three-sided FRP U-wrap or two-opposite-sides strengthening schemes. V_c, which is equal to the shear strength provided by concrete for non-prestressed members in a state that is only under the effect of shear and bending, using Equations (5) and (6), and V_s, which is equal to the nominal shear strength provided by shear bars, according to Equation (7) is derived according to the ACI Committee 440.2R (American Concrete Institute, 2008).

$$V_c = 0.17\sqrt{f_c}\, b_w d \tag{5}$$

$$V_c = \left(0.16\sqrt{f_c} + 17\rho_w \frac{V_u d}{M_u}\right) b_w \tag{6}$$

$$V_s = \frac{A_V f_{yt}(\sin\alpha + \cos\alpha)d}{s} \tag{7}$$

where f_c is specified compressive strength of concrete [MPa], b_w is the width of the web [mm], d is the distance from extreme compression fiber to the centroid of tension reinforcement [mm], M_u is the factored moment at a section [N-mm], V_u is the factored shear force at the section [N], and finally, the ratio $\rho_w = A_s/(b_w d)$ where A_s is the area of nonprestressed steel reinforce-

ment [mm²]. In Equation (7), A_V is the area of shear reinforcement spacing s. Angle α is the angle defining the orientation of reinforcement. f_{yt} is the specified yield strength f_y of transverse reinforcement [MPa].

The contribution of the FRP system to the shear strength of a member is based on the fiber orientation and an assumed crack pattern (Khalifa et al., 1999). The shear strength provided by the FRP reinforcement can be determined by calculating the force resulting from the tensile stress in the FRP across the assumed crack. The shear contribution of the FRP shear reinforcement is then given by Equation (8):

$$V_f = \frac{A_{fv} f_{fe}(\sin\alpha + \cos\alpha)d_{fv}}{s_f} \tag{8}$$

where A_{fv} is the area of FRP shear reinforcement with spacing s_f, whose value is equal to $2nt_f w_f$ [mm²], where n is the number of plies of FRP reinforcement, t_f is the nominal thickness of one ply of FRP reinforcement, and w_f is the width of FRP reinforcing plies [mm]. d_{fv} is the effective depth of FRP shear reinforcement in millimeters, and α is the angle of the FRP shear reinforcement strip with the longitudinal axis of the member. f_{fe} is the effective stress in the FRP, stress level attained at section failure and is obtained from Equation (9):

$$f_{fe} = \varepsilon_{fe} E_f \tag{9}$$

where ε_{fe} is equal to the effective strain and it is calculated according to Equations (10) and (11) according to the different arrangements of FRP sheets.

For reinforced concrete column and beam members completely wrapped by FRP, the loss of aggregate interlock of the concrete has been observed to occur at fiber strains less than the ultimate fiber strain. To preclude this mode of failure, the maximum strain used for design should be limited to the smallest value of 0.004 and 0.75 of the design failure strain (ε_{fu}). In this case, the effective strain is calculated from Equation (10).

$$\varepsilon_{fu} = 0.75\varepsilon_{fu} \leq 0.004 \tag{10}$$

Bonded U-wraps or bonded face plies, FRP systems do not enclose the entire section (two- and three-sided wraps), have been observed to delaminate from the concrete before the loss of aggregate interlock of the section. For this reason, bond stresses have been analyzed to determine the usefulness of these systems (Triantafillou & Plevris, 1992), and the effective strain is obtained according to Equation (11):

$$\varepsilon_{fe} = K_v \varepsilon_{fu} \leq 0.004 \tag{11}$$

It should be noted that in Equations (10) and (11), ε_{fu} is obtained from the product of the reduction factor of the environmental conditions and the ultimate failure

strain reported by the factory. This coefficient is considered equal to 0.95 and 0.75 for mild environmental conditions and the type of carbon and glass fibers, respectively. The bond-reduction coefficient is a function of the concrete strength, the type of wrapping scheme used, and the stiffness of the laminate. It is obtained from Equation (12):

$$K_v = \frac{k_1 k_2 L_e}{11900 \varepsilon_{fu}} \leq 0.75 \tag{12}$$

The active bond length (L_e) is the length over which the majority of the bond stress is maintained. This length is calculated by Equation (13):

$$L_e = \frac{23300}{(n t_f E_f)^{0.58}} \tag{13}$$

The bond-reduction coefficient also relies on two modification factors, k_1 and k_2, that account for the concrete strength and the type of wrapping scheme used, respectively. Calculate k_1 from Equation (14) and calculate k_2, in case a U-wraps stirrup is used, from Equation (15). Equation (16) is used for two sides bonded scheme.

$$k_1 = \left(\frac{f_c'}{27} \right)^{\frac{2}{3}} \tag{14}$$

$$k_2 = \frac{d_{fv} - L_e}{d_{fv}} \tag{15}$$

$$k_2 = \frac{d_{fv} - 2L_e}{d_{fv}} \tag{16}$$

It should be noted that the total shear strength provided by the steel shear reinforcement and the FRP shear reinforcement must follow Equation (17):

$$V_s + V_f \leq 0.66 \sqrt{f_c'} b_w d \tag{17}$$

3.2. Shear strength of FRP-strengthened RC beams – Publication No. 345

Chapter 9 of this guide contains the general criteria for using FRP materials as external stirrups, in order to increase the shear and torsion strength of reinforced concrete sections. Based on this, the final shear strength of the section V_r is calculated using Equation (18):

$$V_r = \varphi_c V_c + \varphi_s V_s + \varphi_{frp} V_{frp} \tag{18}$$

where φ_c, φ_s and φ_{frp} are the partial safety factor of concrete (equal to 0.6), steel equal to (0.85) and FRP material equal to 0.85, respectively. The ultimate shear strength provided by concrete, V_c, and the ultimate

shear strength provided by shear reinforcement, V_s, are obtained from the Iranian concrete code "ABA". The shear strength provided by FRP materials (V_{frp}) is added to include the contribution of the FRP shear reinforcement. V_c and V_s are calculated from Equations (19) and (20):

$$V_c = 0.2 \sqrt{f_c'} b_w d \tag{19}$$

$$V_s = A_V f_y \frac{d}{s} \tag{20}$$

The contribution of FRP material from the shear is determined according to Equations (21) and (22):

$$V_f = \frac{E_{frp} \varepsilon_{frpe} A_{frp} d_{frp} (\sin\beta + \cos\beta)}{s_{frp}} \tag{21}$$

$$A_{frp} = 2 t_{frp} w_{frp} \tag{22}$$

The effective depth of FRP stirrups, d_{frp}, is considered as the distance from extreme compression fiber to centroid of tension reinforcement, and in the case where the section is completely wrapped around, it is assumed to be equal to h (beam height). The effective strain of FRP materials, ε_{frpe}, is obtained through testing and applying Equations (23) and (26), and in any case, the lowest value obtained from the above two methods is considered. But the effective strain ε_{frpe} should be limited to 0.004, because in the higher range of strain, the loss of the aggregate interlock of the concrete has been observed due to the opening of cracks.

$$\varepsilon_{frpe} = R \varepsilon_{frpu} \tag{23}$$

R, the ratio of effective strain to ultimate strain in FRP stirrups is obtained from Equation (24), and the ratio of FRP shear reinforcement, ρ_{frp}, is obtained from Equation (25):

$$R = 0.8 \lambda_1 \left(\frac{f_c^{2/3}}{\rho_{frp} E_{frp}} \right)^{\lambda_2} \tag{24}$$

$$\rho_{frp} = \frac{2 t_{frp} w_{frp}}{b_w s_{frp}} \tag{25}$$

In Equation (24), coefficients λ_1 and λ_2 for carbon fibers are: $\lambda_1 = 1.35$ and $\lambda_2 = 0.3$, aramid fibers and glass: $\lambda_1 = 1.23$ and $\lambda_2 = 0.47$.

$$\varepsilon_{frpu} = \frac{\varphi_{frp} k_1 k_2 L_e}{9525} \tag{26}$$

In order to consider the possibility of debonding of FRP sheets, the effective strain is considered equal

to the lowest three values A, B and C: effective strain limit ε_{frpe}, the value obtained from Equation (10) and the value presented in Equation (11), respectively.

$$k_1 = \left[\frac{f_c^{'}}{27.65}\right]^{\frac{2}{3}} \tag{27}$$

$$k_2 = \frac{d_{frp} - n_e L_e}{d_{frp}} \tag{28}$$

where k_1 is an index of concrete shear strength and k_2 is an index for the type of wrapping scheme. In Equation (28), n_e is the number of free ends of FRP stirrups on one side of the beam. If we have FRP beams on only 2 side faces, $n_e = 2$, and if thP srrup is U-wraps, then $n_e = 1$. When $k_2 \leq 0$, the FRP system is ineffective in sheanless FRP restraint is provided in a suitable manner. The effective restraint length, L_e, is calculated ung Equation (29), which is proposed based on experimental data:

$$L_e = \frac{253350}{(t_{frp} E_{frp})^{0.58}} \tag{29}$$

It should be noted that the ultimate shear strength of the section is limited to the Equation (30):

$$V_r = V_c + V_s + V_{frp} \leq V_c + 0.8\varphi_c \sqrt{f_c^{'}} b_w d \tag{30}$$

3.3. Shear strength of FRP-strengthened RC beams using a neural network

In Figure 4, the neural network architecture used in this research is presented. This feed-forward neural network consists of three layers. Nodes represent neurons, and arrows represent weighted connections. This network includes 11 neurons in the input layer, 10 in the hidden layer, and 1 in the output layer. The number of input and output neurons depends on the problem to be solved, while the number of hidden layers and the number of neurons may be checked by different situations, and the most optimal one is selected. The network training is done by updating the weights related to the connections between neurons based on the known input and the output patterns or learning patterns using aeraverocess. These weights indicate the influence and strength of a connection among neurons.

Considering the many parameters that influence the beam shear failure mode, creating an efficient neural network requires an appropriate selection of input variables. However, it should be kept in mind that increasing the input neurons to a neural network may reduce the accuracy and efficiency of the training process (Kasabov, 1996). In this article, the selection of input parameters is based on the shear capacity relationships that were examined earlier. As a basic idea, the ACI Committee 318M (American Concrete Institute, 2005) regulations specify that three variables have the greatest contribution to the shear strength of concrete, these variables include: $1 - f_c^{'}$, $2 - A_s / b_w d$, $3 - V_u d / M_u$. After counting trial and error, 11 main variables were considered as input to the network (Tab. 1).

In this research, a comprehensive and extensive review of forty articles[1], has been carried out to compile data on 304 reinforced concrete beams reinforced in shear using FRP sheets (Tab. A1, *Appendix A*). These laboratory results have been used to provide a database for the ANN model. The 304 analyzed beam samples are randomly divided into three groups: a) training data set comprising 60% of the total data set (182 data); b) validation data set comprising 20% of the total data set (61 data); c) the test data set consists of 20% of the total data set (61 data).

All beams were simply supported with various span lengths, and they were subjected to two concentrated loads symmetrically placed about the midspan. In the data collection, different schemes of FRP shear strengthening for reinforced concrete beams are considered (Fig. 2) (Completely wrapped, U-wraps or side bonding of the web). The FRP sheets can be applied as intermittent strips (like stirrups) or a continuous sheet along the length of the member. In addition, the parameters available in the laboratory database have a wide range of loading arrangement, sectional geometry, material properties, reinforcement ratio, as well as geometry, arrangement and mechanical properties of FRP external reinforcement. Therefore, we will have a wide range of failure loads.

---

[1] Abdel-Jaber et al., 2003; Adhikary & Mutsuyoshi, 2004; Alzate et al., 2013; Barros & Dias, 2006; Beber & Campos-Filho, 2005; Bousselham & Chaallal, 1988; Bukhari et al., 2010; 2013; Cao et al., 2005; Carolin & Täljsten, 2005; Chaallal et al., 1988; Deniaud & Cheng, 2001; Diagana et al., 2003; Dias & Barros, 2012; Grace et al., 2003; Grande et al., 2009; Islam et al., 2005; Kamiharako et al., 1997; Khalifa et al., 1999; Khalifa & Nanni, 2000, 2002; Kim et al., 2008; Leung et al., 2007; Mofidi & Chaallal, 2014; Mofidi et al., 2014; Monti & Liotta, 2007; Norris et al., 1997; Ozden et al., 2014; Panda et al., 2011; Pellegrino & Modena, 2002, 2008; Saadatmanesh & Ehsani, 1991; Singh, 2013; Sundarraja & Rajamohan, 2009; Täljsten, 2003; Tanarslan et al., 2008; Teng et al., 2009; Umezu et al., 1997; Zhang & Hsu, 2005; Zhang et al., 2004.
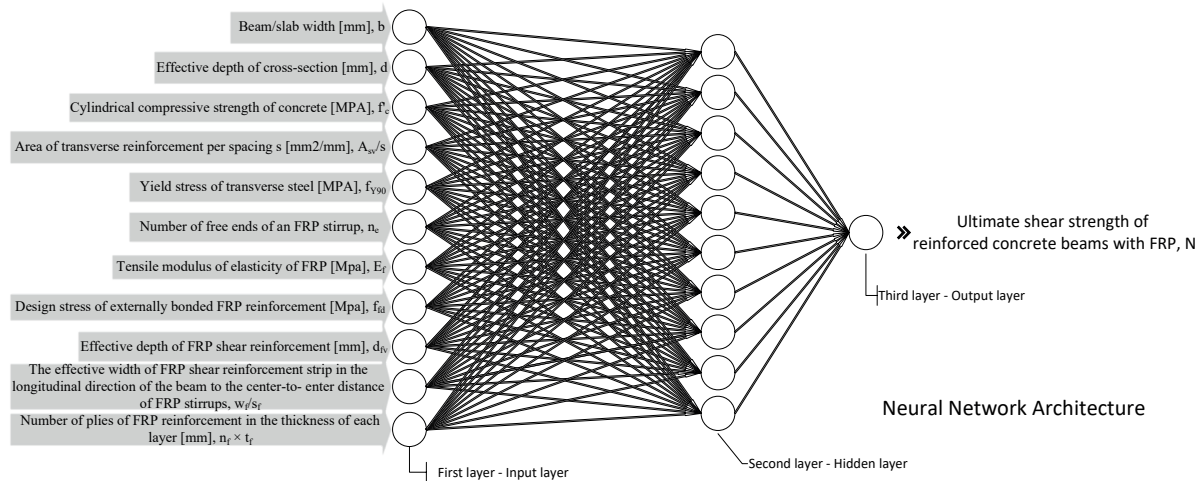
Fig. 4. Schematic diagram of the neural network architecture

In the neural network structure, according to Table 1, all the significant variables in the data are considered input variables for the model. The number of hidden layers was equal to one, and the number of neurons in the hidden layer was chosen equal to 10. Here, the number of neurons in the hidden layer was optionally considered to be 10, it should be noted that more neurons in the hidden layer require more calculations, and if the number is too high, it will cause overfitting of the data. However, a network with more neurons will solve more complex problems (Alwosheel et al., 2018).

Also, in neural network training, the Levenberg–Marquardt backpropagation algorithm is used with a tangent sigmoid transfer function in the hidden layer and a linear transfer function in the output layer. It should be noted that the neural network's performance is based on the Mean Squared Error (MSE) using the MATLAB program. The optimal network was selected based on the lowest error rate and the highest correlation coefficient between the data. The network specifications are given in Table 2.

Table 1. Range of input and output variables

No.	Variable	Symbol	Minimum	Maximum	Average
	Input element				
1	beam/slab width [mm]	b	75.00	600.00	172.09
2	effective depth of cross-section [mm]	d	124.60	720.00	304.10
3	cylindrical compressive strength of concrete [MPa]	f_c'	10.60	71.40	34.80
4	area of transverse reinforcement per spacing s [mm^2/mm]	A_{sy}/s	0.00	2.01	0.24
5	yield stress of transverse steel [MPa]	f_{Y90}	0.00	650.00	225.03
6	number of free ends of an FRP stirrup*	n_e	–	–	–
7	tensile modulus of elasticity of FRP [MPa]	E_f	5.30	640.00	201.23
8	design stress of externally bonded FRP reinforcement [MPa]	f_{fd}	112.00	4500.00	3032.89
9	effective depth of FRP shear reinforcement [mm]**	d_{fy}	80.00	800.00	306.97
10	the effective width of FRP shear reinforcement strip in the longitudinal direction of the beam to the center-to-enter distance of FRP stirrups	w_f/s_f	0.11	1.50	0.73
11	number of plies of FRP reinforcement in the thickness of each layer [mm]	$n_f \times t_f$	0.04	2.10	0.43
	Output element				
1	laboratory ultimate shear strength [N]	V_{U-exp}	45.90	881.20	173.80

* n_e is the number of free ends of the FRP stirrup on the side of the beam (n_e = 2 for side plates, n_e = 1 for a U-wrap, and n_e = 0 for completely wrapped).

** The effective depth of FRP shear reinforcement d_{fy} is taken as the distance from the free end of the FRP shear reinforcement underneath the slab to the bottom of the internal steel stirrups. For the rare case of completely wrapped member, d_{fy} is taken as the total height of the section (Canadian Standard Association, 2002).

Table 2. Network specifications

No.	Parameter	Specifications	R	MSE
1	Network function	feed-forward backprop with Trainlm (Levenberg–Marquardt backpropagation) as a training function	R	MSE
2	Network structure	11-10-1		
3	Number of training data	182	0.991	296.29
4	Number of validation data	61	0.969	700.13
5	Number of test data	61	0.946	964.38
6	Number of all data	304	0.981	511.38

3.3.1. Efficiency criteria of models

There are various indicators to evaluate the performance of estimation and forecasting models. In the following section, the criteria for measuring the number of prediction errors will be discussed.

The correlation coefficient R expresses the degree of correlation between the estimated results of the model and the real data, which is calculated based on Equation (31). In fact, the correlation coefficient measures the linear relationship between two variables, obviously, the closer its value is to one, the closer the estimated values are to the actual values.

$$R = \frac{\sum_{i=1}^{n}(V_{e,i} - \overline{V}_e)(V_{p,i} - \overline{V}_e)}{\left[\sum_{i=1}^{n}(V_{e,i} - \overline{V}_e)^2 \sum_{i=1}^{n}(V_{p,i} - \overline{V}_e)^2\right]^{0.5}} \quad (31)$$

The performance indicators used are the Mean Absolute Relative Error (MARE), Mean Absolute Error (MAE), Mean Squared Error (MSE), Root Mean Squared Error (RMSE), and Root Mean Squared Relative Error (RRMSE). These are calculated using Equations (32)–(36), and can range from zero (indicating excellent performance) to infinity (indicating very poor performance).

$$MARE = \frac{1}{n}\sum_{i=1}^{n}\frac{\left|V_{e,i} - V_{p,i}\right|}{V_{e,i}} \times 100 \quad (32)$$

$$MAE = \frac{\sum_{i=1}^{n}\left|V_{e,i} - V_{p,i}\right|}{n} \quad (33)$$

$$MSE = \frac{\sum_{i=1}^{n}(V_{e,i} - V_{p,i})^2}{n} \quad (34)$$

$$RMSE = \sqrt{MSE} \quad (35)$$

$$RRMSE = \frac{RMSE}{\overline{V}_e} \quad (36)$$

In the above relationships, $V_{e,i}$ is the laboratory shear values, $\overline{V}_e$ is the average laboratory shear values, $V_{p,i}$ is the predicted shear values by regulation relations or neural network model and $\overline{V}_p$ is the average predicted shear values. n is the number of exaned samples.

3.3.2. Comparison of neural network architectures

The environment used to build neural networks is MATLAB R2013b. It will be possible to compare the architecture of neural networks by running nntool toolbox and addressing input and output data (an 11 × 304 input data matrix that represents 304 samples of 11 elements and an 1 × 304 output data matrix that represents 304 samples of 1 element. These input and output elements are listed in Table 1).

By considering feed-forward backprop network type, there will be a wide range of learning functions. A comparison of all learning functions and corresponding performance results are listed in Table 3. Note that as a primary solution, the default values for the nntool toolbox were selected as follows: MSE as a performance function, tansig (tangent sigmoid transfer function) as a transfer function, two-layer network and ten hidden neurons. The MATLAB toolbox does not refer to the inputs as a layer. Therefore, a two-layer network means a network that consists of an output layer, a hidden layer plus an input layer, as shown in Figure 3. In this section, learning and transfer functions are discussed, and in the next section, the number of layers and the number of hidden neurons are discussed in ANN complexity adjustment.

As can be seen in Table 3, the best performance results are obtained by Trainbr (Bayesian regularization backpropagation) and Trainlm (Levenberg–Marquardt backpropagation) learning functions. Both of these learning functions update the weight and bias values according to Levenberg–Marquardt optimization, but the Trainlm function is faster than the Trainbr function and is often even the fastest backpropagation algorithm in the toolbox, although it does require more memory than other algorithms. Therefore, by choosing Trainlm as the training function, other effective parameters will be investigated.

Table 3. Comparison of all learning functions and corresponding performance results using nntool – MATLAB R2013b toolbox

Training function	MSE	R	Training function	MSE	R
Trainbfg: BFGS quasi-Newton back-propagation	2041.51	0.933	Traingda: Gradient descent with adaptive learning rate backpropagation	26520.96	$1.853e^{-26}$
Trainbr[1]: Bayesian regularization backpropagation	435.59	0.975	Traingdx: Gradient descent with momentum and adaptive learning rate backpropagation	22076.16	$1.853e^{-26}$
Traincgb: Conjugate gradient backpropagation with Powell–Beale restarts	1118.55	0.949	Trainlm[2]: Levenberg–Marquardt backpropagation	511.38	0.981
Traincgf: Conjugate gradient backpropagation with Fletcher–Reeves updates	1772.57	0.912	Trainoss: One-step secant backpropagation	1005.10	0.954
Traincgp: Conjugate gradient backpropagation with Polak–Ribiére updates	1610.26	0.930	Trainr[3]: Random order incremental training with learning functions	take a long time	–
Traingd: Gradient descent backpropagation	77763.62	–0.117	Trainrp: Resilient backpropagation	1225.23	0.920
Traingdm: Gradient descent with momentum backpropagation	253100.80	0.338	Trainscg: Scaled conjugate gradient backpropagation	1244.57	0.950

[1] Trainbr: is a network training function that updates the weight and bias values according to Levenberg–Marquardt optimization. It minimizes a combination of squared errors and weights, and then determines the correct combination so as to produce a network that generalizes well. The process is called Bayesian regularization.

[2] Trainlm: is a network training function that updates weight and bias values according to Levenberg–Marquardt optimization.

[3] Trainr: trains a network with weight and bias learning rules with incremental updates after each presentation of an input. Inputs are presented in random order.

Three transfer functions can be selected for each layer (tan-sigmoid, log-sigmoid and linear transfer function – Fig. 5). Therefore, in a two-layer network, there will be a total of 9 choices for the transfer functions. A network of two layers, where the first layer is tangent sigmoid and the second layer is linear, can be shown to have the best performance results.

a)

b)

c)
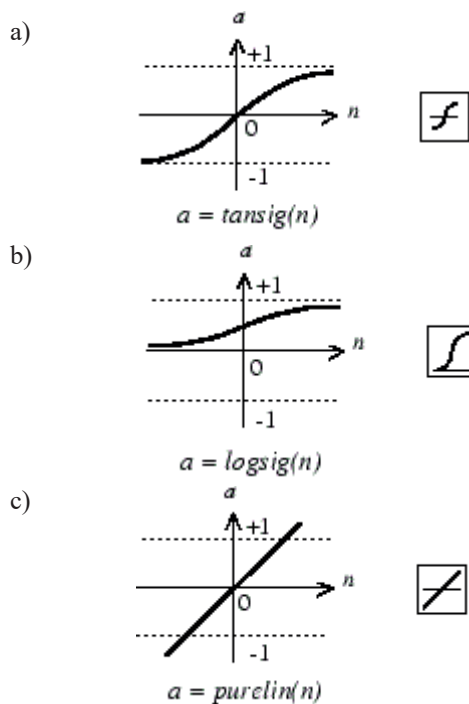
Fig. 5. Transfer Function Diagrams: a) tan-sigmoid transfer function; b) log-sigmoid transfer function; c) linear transfer function

3.3.3. ANN complexity adjustment

For the number of hidden layers and the number of hidden neurons, different choices lead to ANN with different levels of complexity. For example, adding more neurons to a particular hidden layer increases the network's capacity because it has more degrees of freedom.

An ANN's training process aims to produce a model that approximates the underlying data generating process (DGP) based on previous observations (so-called training data). A successful approximation of the underlying process implies that the trained network is generalizable, meaning that it maintains a consistent performance in the available data used for training and on future data generated by the same DGP. Importantly, an ANN may fail to deliver such performance consistency if the network is excessively complex compared to the underlying data generating process. In this case, ANN performs very well the training data, but fails to maintain a similarly strong performance on different data generated by the same DGP, which are used for validation purposes (so-called validation data). This issue is known as overfitting. Another issue that may impact the extent to which a trained ANN's is generalizable is known as underfitting, which means that the ANN is too sple compared to the underlying DGP. As a result, it performs poorly on both training and validation data. In this case, the ANN cannot accurately capture the relation (embodied in the DGP) between input and observed choices. In sum, it is essential for the analyst to consider the relation between

complexity and performance. The above-described concepts of under- and overfitting a learning machine are shown in Figure 6 (Alwosheel et al., 2018).

Low model complexity (compared to the underlying DGP) is represented in Figure 6 on the left-hand side: here, models perform poorly on both training and future data, as they impose assumptions that are too simplistic on the DGP. In contrast, very complex models are represented on the right hand side. These models perform well on the available data, but fail to obtain a similarly strong performance on validation data generated by the same DGP. The ideal level of complexity is found in the range where the validation error is low, and the divergence between training and validation error (thus the vertical distance between the red and green lines) is small (Alwosheel et al., 2018).

This section adjusts the ANN complexity by adding/removing hidden neurons and the number of hidden layers. For example, if the underlying DGP is complex, an ANN with very few hidden neurons (in the extreme case: only one hidden neuron) will underfit this DGP. In contrast, using a large number of hidden neurons will lead to overfitting. Various ANNs with different levels of complexity (i.e., different number of hidden neurons) are estimated using the training set. Then, the performance of each of the estimated ANNs is evaluated on the validation set. The network that has the best performance with respect to the validation set is selected, as its complexity falls in the ideal level of complexity range shown in Figure 6. Subsequently, to provide an unbiased evaluation of the selected network, ANN performance is further evaluated on the testing set. If the ANN also performs well on the testing data, the analyst can be confident that the network has successfully learned the underlying DGP[2] (Alwosheel et al., 2018).

Figure 7 shows the relationship between ANN complexity (i.e., the number of hidden neurons) and the correlation coefficient R obtained on training, validation, and test datasets. The network that provides the best performance on the validation data is then selected. Figure 7 shows that ten hidden neurons provide the best performance (on the validation set). Using more

than ten hidden neurons does not affect the resulting correlation coefficient R, implying that ANN has learned the input/output relationship with ten neurons. According to Occam's razor principle, an explanation of a set of data should be limited to the bare minimum that is consistent with the data (Alwosheel et al., 2018). In Figure 7, increasing the complexity does not result in better performance. Therefore, the simplest model that describes data is preferred, which in this case is an ANN with ten neurons.
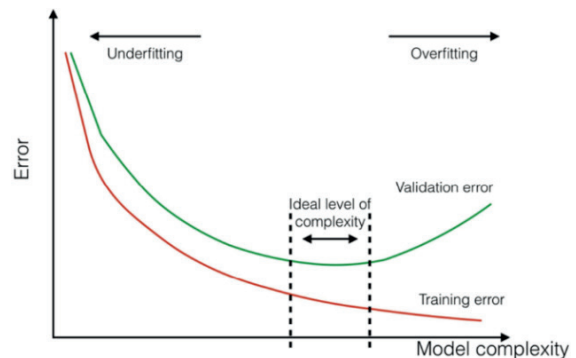
Fig. 6. A conceptual representation of the relationship between model complexity and performance
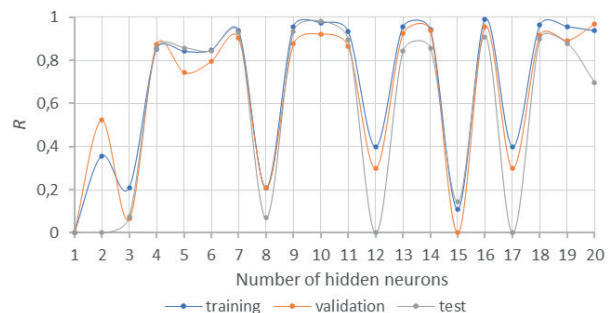
Fig. 7. Number of ANN hidden neurons vs the correlation coefficient R values for training, validation, and test datasets

Note that a different number of hidden layers have also been implemented for this study. By choosing the 3-layer network (Fig. 3), it can be shown in a similar way that adding more hidden layers does not improve the prediction performance.

It is expected that the more complex the ANN is, the more data will be needed for training the network, leading to a larger sample size (Alwosheel et al., 2018). Therefore, according to what was ateempted by choosing a network with 3-layers and 10 hidden neurons, the complexity of the network falls in the ideal level of complexity range shown in Figure 6, where the validation error is low, and the divergence between training and validation error is small.

---

[2] In some cases, training the ANN and adjusting its complexity may not result in a low generalization error, which means that the ANN has failed to approximate the underlying DGP to a sufficient extent. One possible reason of this outcome is that the used data are insufficient in size; i.e., when trained on a very small dataset – relative to the number of nodes in the network – the ANN may end up memorizing observations rather than learning the underlying DGP. In this case, it is recommended to use larger datasets (Alwosheel et al., 2018).

4. Presentation of results

Table 4 shows the neural network model's performance criteria and two Iranian and American regulations for all data.

Table 4 calculated from a comparison of design shear strength values obtained by ACI 440.2R-08 and ACI 318-08, design shear strength values obtained by Publication No. 345 – ABA and shear strength values obtained by neural network model with actual experimental shear strength values measured in the laboratory, as it is shown in Table A1 (*Appendix A*).

As it is clear from Table 4, all efficiency criteria for the neural network model are better compared to both regulations, so that, for example, the correlation coefficient of the neural network model is close to 1, while this criterion does not have suitable values for the two regulations. Also, in the comparison of the two regulations, considering all efficiency criteria, the results of the American regulations are more accurate than the Iranian regulations.

Figure 8a–c shows the predicted values of the neural network model compared to its actual (laboratory) values, respectively, for three categories of training, validation, and testing datasets. Figure 8d shows the predicted values of the neural network model compared to its actual values for all data.

Table 4. Performance criteria of shear strength estimation models for all data

Relationship/model	Equation	MARE [%]	MAE	MSE	RMSE	RRMSE	R
ACI 318-05 and ACI 440.2 (2008)	(3)	34.24	62.13	7261.52	85.21	0.49	0.8419
Publication No. 345 – ABA	(18)	38.94	69.93	8268.94	94.70	0.55	0.8418
ANN MODEL	model	13.46	16.97	511.38	22.61	0.13	0.9811
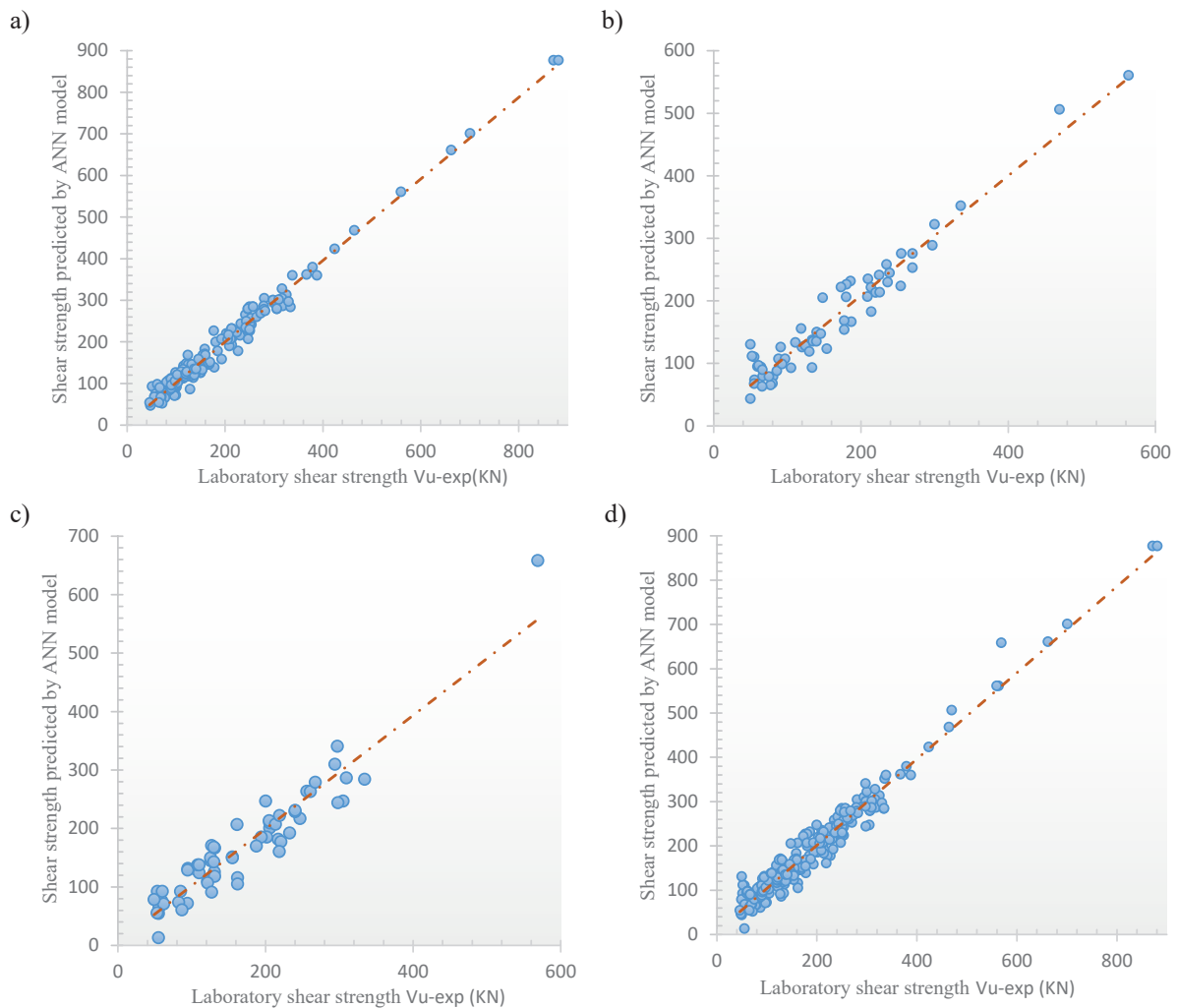
Fig. 8. Comparison of laboratory shear strength V_{U-exp} (KN) with shear strength predicted by ANN model for:
a) training data; b) validation data; c) test data; d) all data

In Figures 8a–c, the diagonal axis shown is located where the predicted and experimental values have the same value. Therefore, the density of points around the diagonal axis shows more accurate predicted values. As expected, a better prediction has been obtained for the training data set compared to the other two sets, and the dispersion of the data around the diagonal axis is less in this set.

Figure 9 presents the graph of the actual shear strength values compared to the output of the regulations and the neural network model for all 304 data is presented. As it is clear from the diagram, the neural network model benefits from more agreement with the real values compared to the output of the regulations.

Table 5 has been prepared to evaluate and compare the relationship between Iranian and American regulations, as well as the neural network prediction model in the use of all types of FRP wrapping schemes (completely wrapped, U-wraps or side bonding of the web, each applied as intermittent strips or a continuous sheet along the length of the member). All the data are placed in their specific wrapping schemes and using performance indicators, the error between the output values of the regulations or the neural network model and its actual values has been estimated.
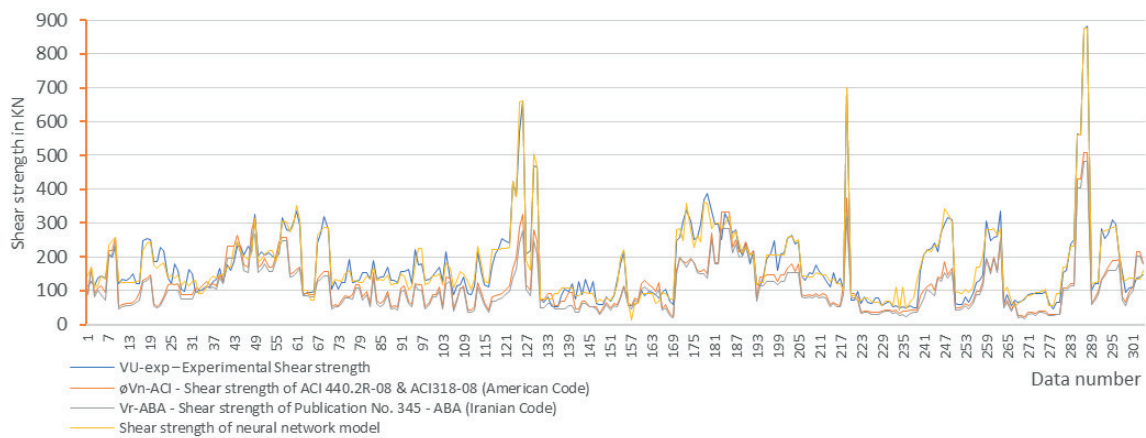
Fig. 9. Experimental shear strength compared to ANN model and regulations codes for all data

Table 5. Comparison of the relations between Iranian and American regulations, as well as the prediction model of ANN in the use of various types of FRP wrapping schemes

Relationship/model	MARE [%]	MAE	MSE	RMSE	RRMSE	R
ACI 318-05 and ACI 440.2 (2008)						
Side bonding – discrete strips	27.1	29.6	1541.3	39.3	0.39	0.410
Side bonding – continuous sheet	32.2	50.2	3725.1	61.0	0.38	0.820
U-wrap – discrete strips	33.9	50.7	4286.8	65.5	0.44	0.890
U-wrap – continuous sheet	32.5	62.1	6498.8	80.6	0.43	0.830
Completely wrapped – discrete strips	40.1	91.8	14565.6	120.7	0.53	0.900
Completely wrapped – continuous sheet	46.9	130.9	24436.7	156.3	0.56	0.660
Publication No. 345 – ABA						
Side bonding – discrete strips	35.2	38.4	2302.2	48.0	0.48	0.440
Side bonding – continuous sheet	35.2	54.5	4342.2	65.9	0.41	0.840
U-wrap – discrete strips	39.1	56.8	5149.3	71.8	0.48	0.890
U-wrap – continuous sheet	36.5	71.6	8739.2	93.5	0.50	0.790
Completely wrapped – discrete strips	44.9	102.1	17256.3	131.4	0.58	0.910
Completely wrapped – continuous sheet	50.5	142.8	30185.0	173.7	0.62	0.660
Neural network model						
Side bonding – discrete strips	12.8	11.0	210.4	14.5	0.14	0.900
Side bonding – continuous sheet	13.1	17.6	576.1	24.0	0.15	0.960
U-wrap – discrete strips	19.1	17.5	555.1	23.6	0.16	0.970
U-wrap – continuous sheet	10.4	16.1	429.2	20.7	0.11	0.979
Completely wrapped – discrete strips	11.1	18.4	509.6	22.6	0.10	0.990
Completely wrapped – continuous sheet	10.8	23.5	938.2	30.6	0.11	0.978

Figure 10 graphically shows the prediction error of the neural network model, the Iranian and American regulations according to Mean Squared Error (MSE) for different types of FRP wrapping schemes. From Table 5 and Figure 10, it can be concluded that in all the data and in all the beam shear strengthening patterns in all cases, the neural network model has the lowest estimation error by a large difference from the others, and it shows that the output of this model is closer to the real values. After the artificial neural network model, the estimated values of the relationship of the American regulation predict a lower estimation error than its corresponding Iranian relationship. In the American and Iranian regulations, as well as in the neural network model, from a general point of view and ignoring the type of applying FRP laminates (intermittent strips or a continuous sheet), the lowest amount of estimation error belongs to the side bonding of the beam, followed by the U-wraps stirrup and at the end the completely wrapped. In the case that, the beam is strengthened with a completely wrapped scheme, the regulations show the highest amount of error, one of the main reasons for that is limiting the total shear capacity of the steel and FRP shear reinforcement to $0.66\sqrt{f_c'}b_w d$ for the relationship of the ACI 318-05 and ACI 440.2 and the value of $4 \times 0.2 \times \sqrt{f_c'}b_w$ for the relation of Publication No. 345. This is despite the fact that in such cases, the real shear strength is higher than what the regulations predict. It is worth mentioning that in all wrapping schemes, where the FRP system is installed in the form of intermittent strips (discrete strips), the regulatory relations show a lower error value than the similar case of a continuous sheet along the length of the member.
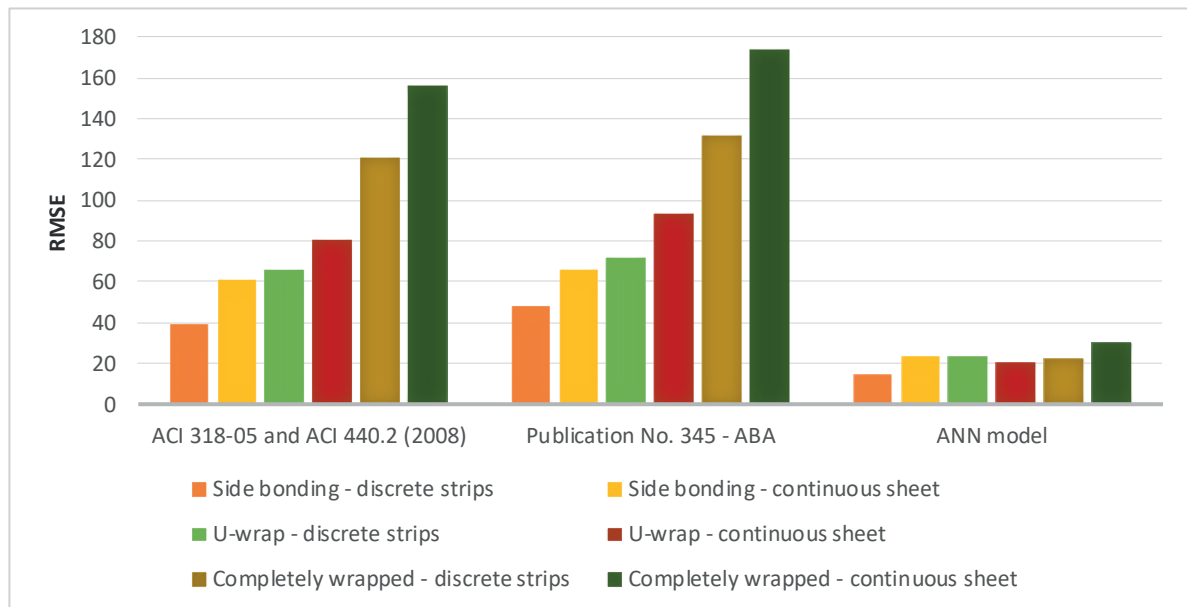
Fig. 10. Comparison of the prediction error of various FRP wrapping schemes in the regulations and the neural network model

5. Conclusion

In this study, the shear strength of RC beams reinforced by FRP with different wrapping schemes has been investigated by artificial neural network. To model the neural network, beam width, beam height, compressive strength of concrete, the ratio of the area of transverse reinforcements to the distances between them, the yield stress of transverse reinforcements, the number of free ends of FRP stirrups, FRP modulus of elasticity, strength tensile FRP, the effective depth of FRP stirrups, the effective width of the FRP shear reinforcement strip in the longitudinal direction of the beam to the center-to-center distance of the FRP stirrups, the number of FRP layers multiplied by the thickness of each layer as 11 input variables and the value of the total shear strength of the beam as a variable output were all considered.

By comparing the results based on the efficiency criteria of the data-based models, it can be concluded that in all types FRP wrapping schemes (completely wrapped, U-wraps or side bonding of the web, each applied as intermittent strips or a continuous sheet along the length of the member), the neural network model has the lowest error by a large difference from the others, and after that, the relationship of the American

concrete code ACI 440.2R is in the second place with less error than its corresponding Iranian relationship. Specifically, the values of the correlation coefficient for an artificial neural network, American concrete code and Iranian concrete code are 0.9811, 0.8419 and 0.8418, respectively. In addition, the percentage of the Mean Absolute Relative Error (MARE) in the neural network model is about 13%, which is 21% and 26% less than the results of the American and Iranian regulations. In addition, in all three wrapping schemes, from a general point of view and ignoring the type of applying FRP laminates (intermittent strips or a continuous sheet), the lowest amount of estimation error belongs to the side bonding of the beam, followed by the U-wraps stirrup and finally the completely wrapped. Finally, it can be said that it is difficult to create a general model to estimate the shear strength due to the complexity of the shearing mechanism of concrete beams and the various parameters affecting it. Therefore, the exact values of shear strength are not available. Regulations such as American concrete regulations and Iranian concrete regulations each use empirical formulas provided for a set of specific data, but using a neural network model using a set of laboratory data has greater accuracy in estimating shear strength.

Data availability

Data will be available upon reasonable request.

Conflict of interest

There is no conflict of interest to declare.

Appendix A

Table A1. Ultimate experimental shear strength measured in the laboratory (a), design shear strength values obtained by ACI 440.2R-08 and ACI 318-08 (b), design shear strength values obtained by Publication No. 345 – ABA (c) and shear strength values obtained by neural network model (d)

	a) Experimental	b) ACI 440.2R-08 and ACI318-08										c) Publication No. 345 – ABA												d) ANN
No.	$V_{U\text{-}exp}$	V_c	V_s	L_e	K_1	K_2	K_v	ε_{fe}	V_f	Check Equation (17)	$\varnothing V_{n\text{-}ACI}$	V_c	ρ_{frp}	R	$\varepsilon_{ffpe\text{-}1}$	L_e	K_1	K_2	$\varepsilon_{frpe\text{-}2}$	Min. ε_{frpe}	V_{frp}	Check Equation (30)	$V_{r\text{-}ABA}$	V_{ANN}
1	115.4	53.4	0.0	33.5	1.707	0.781	0.255	0.0035	69.4	69.4	95.6	62.9	0.0018	0.401	0.0059	36.4	1.680	0.761	0.0032	0.0032	61.8	50.1	87.8	142.1
2	127.0	53.4	0.0	33.5	1.707	0.781	0.255	0.0035	172.6	172.6	170.1	62.9	0.0045	0.305	0.0045	36.4	1.680	0.761	0.0032	0.0032	153.6	124.4	162.1	170.9
3	115.4	53.4	0.0	33.5	1.707	0.561	0.183	0.0027	64.5	64.5	92.0	62.9	0.0045	0.305	0.0045	36.4	1.680	0.523	0.0022	0.0022	52.7	42.7	80.4	112.5
4	135.6	53.4	0.0	///	///	///	///	0.0040	78.3	78.3	108.6	62.9	0.0018	///	///	///	///	///	0.0040	0.0040	78.3	63.4	101.1	113.6
5	144.3	53.4	0.0	33.5	1.707	0.781	0.255	0.0035	97.2	97.2	115.7	62.9	0.0018	0.401	0.0059	36.4	1.680	0.761	0.0032	0.0032	61.8	50.1	87.8	142.1
6	138.5	45.8	0.0	33.5	1.387	0.781	0.207	0.0029	79.0	79.0	96.0	53.8	0.0018	0.377	0.0055	36.4	1.365	0.761	0.0026	0.0026	50.2	40.7	73.0	134.1
7	209.5	69.8	66.2	49.5	1.014	0.856	0.201	0.0036	140.7	206.9	217.2	82.1	0.0016	0.361	0.0065	53.8	0.998	0.843	0.0031	0.0031	121.0	154.2	203.5	235.2
8	200.0	69.8	66.2	33.1	1.014	0.903	0.142	0.0025	142.0	208.1	218.2	82.1	0.0031	0.293	0.0053	36.0	0.998	0.895	0.0022	0.0022	121.5	154.7	204.0	246.7
9	234.8	69.8	66.2	26.2	1.014	0.924	0.114	0.0021	195.8	262.0	257.1	82.1	0.0047	0.260	0.0047	28.5	0.998	0.917	0.0018	0.0018	168.0	192.3	241.6	258.2
10	120.9	50.4	0.0	65.1	1.097	0.702	0.281	0.0040	15.4	15.4	53.9	59.2	0.0005	0.518	0.0078	70.8	1.080	0.676	0.0035	0.0035	13.5	10.9	46.5	125.8
11	134.5	50.4	0.0	65.1	1.097	0.702	0.281	0.0040	22.1	22.1	58.8	59.2	0.0007	0.464	0.0070	70.8	1.080	0.676	0.0035	0.0035	19.4	15.7	51.3	125.1
12	131.1	50.4	0.0	65.1	1.097	0.702	0.281	0.0040	26.6	26.6	62.0	59.2	0.0009	0.440	0.0066	70.8	1.080	0.676	0.0035	0.0035	23.3	18.9	54.4	125.0
13	135.7	50.4	0.0	65.1	1.097	0.702	0.281	0.0040	26.8	26.8	62.2	59.2	0.0009	0.438	0.0066	70.8	1.080	0.676	0.0035	0.0035	23.5	19.0	54.6	125.0
14	150.6	50.4	0.0	65.1	1.097	0.702	0.281	0.0040	31.0	31.0	65.2	59.2	0.0010	0.420	0.0063	70.8	1.080	0.676	0.0035	0.0035	27.2	22.0	57.6	125.2
15	120.0	50.4	0.0	65.1	1.097	0.702	0.281	0.0040	44.3	44.3	74.8	59.2	0.0014	0.377	0.0057	70.8	1.080	0.676	0.0035	0.0035	38.8	31.4	67.0	126.0
16	121.7	50.4	0.0	43.5	1.097	0.801	0.214	0.0031	69.6	69.6	93.1	59.2	0.0058	0.249	0.0037	31.7	1.080	0.855	0.0020	0.0020	43.9	35.6	71.1	129.5
17	246.7	50.4	84.4	65.1	1.097	0.702	0.281	0.0040	22.1	106.6	130.6	59.2	0.0007	0.464	0.0070	70.8	1.080	0.676	0.0035	0.0035	19.4	87.5	123.0	216.8
18	253.9	50.4	84.4	65.1	1.097	0.702	0.281	0.0040	31.0	115.4	137.0	59.2	0.0010	0.420	0.0063	70.8	1.080	0.676	0.0035	0.0035	27.2	93.8	129.3	241.9
19	250.6	50.4	84.4	65.1	1.097	0.702	0.281	0.0040	44.3	128.7	146.5	59.2	0.0014	0.377	0.0057	70.8	1.080	0.676	0.0035	0.0035	38.8	103.2	138.7	243.9
20	185.0	28.6	19.1	///	///	///	///	0.0040	24.9	44.0	60.6	33.6	///	///	///	///	///	///	0.0040	0.0040	24.9	36.4	56.6	177.7
21	187.0	28.6	19.1	///	///	///	///	0.0040	16.6	35.7	53.9	33.6	///	///	///	///	///	///	0.0040	0.0040	16.6	29.7	49.8	166.3
22	227.0	28.6	19.1	///	///	///	///	0.0040	24.9	44.0	60.6	33.6	///	///	///	///	///	///	0.0040	0.0040	24.9	36.4	56.6	177.7
23	217.0	28.6	19.1	///	///	///	///	0.0040	49.9	69.0	80.8	33.6	///	///	///	///	///	///	0.0040	0.0040	49.9	56.6	76.8	181.6
24	136.0	28.4	102.0	///	///	///	///	0.0040	26.0	128.0	117.7	33.4	///	///	///	///	///	///	0.0040	0.0040	26.0	103.3	100.1	138.6
25	121.0	28.4	102.0	///	///	///	///	0.0040	13.0	115.0	121.3	33.4	///	///	///	///	///	///	0.0040	0.0040	13.0	95.0	100.1	147.6
26	178.0	28.4	102.0	///	///	///	///	0.0040	26.0	128.0	117.7	33.4	///	///	///	///	///	///	0.0040	0.0040	26.0	103.3	100.1	138.6
27	161.0	28.4	102.0	///	///	///	///	0.0040	13.0	115.0	121.3	33.4	///	///	///	///	///	///	0.0040	0.0040	13.0	95.0	100.1	147.6
28	104.0	21.4	102.0	///	///	///	///	0.0040	6.4	108.4	88.9	25.2	///	///	///	///	///	///	0.0040	0.0040	6.4	90.8	75.6	115.9
29	99.0	21.4	102.0	///	///	///	///	0.0040	3.2	105.2	88.9	25.2	///	///	///	///	///	///	0.0040	0.0040	3.2	88.7	75.6	126.1
30	162.0	21.4	102.0	///	///	///	///	0.0040	6.4	108.4	88.9	25.2	///	///	///	///	///	///	0.0040	0.0040	6.4	90.8	75.6	115.9
31	150.0	21.4	102.0	///	///	///	///	0.0040	3.2	105.2	88.9	25.2	///	///	///	///	///	///	0.0040	0.0040	3.2	88.7	75.6	126.1
32	95.0	55.7	42.4	32.1	0.536	0.895	0.161	0.0013	33.8	76.2	107.9	65.6	0.0009	0.301	0.0024	34.9	0.527	0.886	0.0011	0.0011	28.9	59.5	98.8	131.4
33	100.0	55.7	42.4	32.1	0.536	0.790	0.143	0.0011	29.8	72.3	105.0	65.6	0.0009	0.301	0.0024	34.9	0.527	0.771	0.0010	0.0010	25.2	56.5	95.8	90.9
34	101.0	55.7	42.4	32.1	0.536	0.791	0.143	0.0011	42.5	85.0	114.2	65.6	0.0009	0.301	0.0024	34.9	0.527	0.773	0.0010	0.0010	35.9	65.2	104.5	91.4
35	112.5	55.7	42.4	32.1	0.536	0.786	0.142	0.0011	58.4	100.9	125.7	65.6	0.0018	0.245	0.0020	34.9	0.527	0.767	0.0010	0.0010	49.3	76.0	115.3	111.9

No.	V_{U-exp}	V_c	V_s	L_e	K_1	K_2	K_v	ε_{fe}	V_f	Check Equation (17)	$\varnothing V_{n-ACI}$	V_c	ρ_{frp}	R	ε_{frpe-1}	L_e	K_1	K_2	ε_{frpe-2}	Min. ε_{frpe}	V_{frp}	Check Equation (30)	V_{r-ABA}	V_{ANN}
36	111.0	55.7	42.4	32.1	0.536	0.898	0.162	0.0013	47.9	90.3	118.0	65.6	0.0009	0.301	0.0024	34.9	0.527	0.889	0.0011	0.0011	41.0	69.2	108.6	133.2
37	126.0	55.7	42.4	21.4	0.536	0.931	0.112	0.0009	53.5	96.0	122.1	65.6	0.0026	0.217	0.0017	23.3	0.527	0.925	0.0008	0.0008	45.8	73.2	112.5	144.9
38	133.5	55.7	42.4	21.4	0.536	0.925	0.112	0.0009	43.2	85.6	114.7	65.6	0.0026	0.217	0.0017	23.3	0.527	0.919	0.0008	0.0008	36.9	65.9	105.3	137.4
39	167.0	55.7	42.4	32.1	0.536	0.893	0.161	0.0013	93.8	136.3	151.2	65.6	0.0018	0.245	0.0020	34.9	0.527	0.884	0.0011	0.0011	80.3	101.1	140.4	145.5
40	125.0	55.7	42.4	32.1	0.536	0.893	0.161	0.0013	66.4	108.8	131.4	65.6	0.0018	0.245	0.0020	34.9	0.527	0.884	0.0011	0.0011	56.8	82.0	121.4	145.5
41	177.3	55.7	42.4	///	///	///	///	0.0040	218.4	260.8	231.3	65.6	///	///	///	///	///	///	0.0040	0.0040	216.2	210.7	196.7	168.1
42	158.5	55.7	42.4	///	///	///	///	0.0040	218.4	260.8	231.3	65.6	///	///	///	///	///	///	0.0040	0.0040	218.4	212.4	196.7	168.1
43	186.1	55.7	42.4	///	///	///	///	0.0040	436.8	479.2	231.3	65.6	///	///	///	///	///	///	0.0040	0.0040	436.8	388.7	196.7	231.4
44	232.4	93.4	40.2	36.0	1.234	0.880	0.219	0.0033	207.8	248.0	263.7	109.9	0.0035	0.296	0.0044	39.1	1.214	0.870	0.0028	0.0028	177.4	177.9	243.8	243.8
45	230.8	81.4	40.2	36.0	1.025	0.880	0.182	0.0027	172.6	212.8	228.0	95.7	0.0035	0.280	0.0042	39.1	1.009	0.870	0.0023	0.0023	147.4	153.5	211.0	215.6
46	205.8	76.0	40.2	36.0	0.936	0.880	0.166	0.0025	105.1	145.3	174.7	89.5	0.0023	0.307	0.0046	39.1	0.921	0.870	0.0021	0.0021	89.7	106.9	160.5	200.6
47	232.6	73.1	40.2	36.0	0.889	0.880	0.158	0.0024	99.8	140.0	168.4	86.1	0.0023	0.302	0.0045	39.1	0.875	0.870	0.0020	0.0020	85.2	103.2	154.8	192.2
48	213.8	85.1	40.2	36.0	1.089	0.871	0.191	0.0029	237.7	277.9	278.3	100.2	0.0035	0.285	0.0043	39.1	1.072	0.859	0.0024	0.0024	202.8	198.4	258.5	207.4
49	325.3	76.0	40.2	///	///	///	///	0.0040	354.4	394.6	315.6	89.5	///	///	///	///	///	///	0.0040	0.0040	354.4	320.3	268.4	313.4
50	201.5	69.6	40.2	50.2	0.831	0.833	0.188	0.0029	104.1	144.3	168.5	81.9	0.0020	0.312	0.0048	54.6	0.818	0.818	0.0025	0.0025	88.4	105.7	154.9	185.4
51	213.7	73.0	40.2	50.2	0.887	0.833	0.201	0.0031	111.1	151.2	176.5	85.9	0.0020	0.318	0.0049	54.6	0.873	0.818	0.0026	0.0026	94.3	110.5	162.1	192.3
52	205.5	81.4	40.2	50.2	1.025	0.833	0.232	0.0036	128.3	168.5	196.0	95.7	0.0020	0.332	0.0051	54.6	1.009	0.818	0.0031	0.0031	108.9	122.4	179.8	209.6
53	212.1	84.5	40.2	50.2	1.078	0.833	0.244	0.0038	90.0	130.2	171.0	99.4	0.0013	0.381	0.0059	54.6	1.061	0.818	0.0032	0.0032	76.4	96.0	155.7	219.8
54	202.9	84.5	40.2	50.2	1.078	0.833	0.244	0.0038	90.0	130.2	171.0	99.4	0.0013	0.381	0.0059	54.6	1.061	0.818	0.0032	0.0032	76.4	96.0	155.7	219.8
55	194.2	69.6	40.2	50.2	0.831	0.833	0.188	0.0029	147.2	187.4	199.7	81.9	0.0020	0.312	0.0048	54.6	0.818	0.818	0.0025	0.0025	124.9	135.4	184.5	185.4
56	209.3	85.1	40.2	50.2	1.089	0.833	0.247	0.0038	192.8	233.0	245.8	100.2	0.0020	0.338	0.0052	54.6	1.072	0.818	0.0032	0.0032	163.7	166.7	226.8	218.1
57	316.4	73.1	40.2	///	///	///	///	0.0040	199.6	239.8	257.5	86.1	///	///	///	///	///	///	0.0040	0.0040	199.6	195.8	247.5	304.8
58	280.5	73.0	40.2	///	///	///	///	0.0040	199.6	239.8	257.4	85.9	///	///	///	///	///	///	0.0040	0.0040	199.6	195.8	247.4	304.5
59	275.4	52.5	84.4	20.9	1.160	0.931	0.146	0.0019	47.4	131.8	150.6	61.8	0.0060	0.331	0.0043	22.7	1.142	0.925	0.0016	0.0016	40.7	104.7	141.8	272.6
60	300.3	52.5	84.4	20.9	1.160	0.937	0.147	0.0019	51.6	136.1	153.7	61.8	0.0060	0.331	0.0043	22.7	1.142	0.931	0.0016	0.0016	44.4	107.7	144.8	292.9
61	335.7	52.5	84.4	20.9	1.160	0.949	0.148	0.0019	64.4	148.9	163.0	61.8	0.0060	0.331	0.0043	22.7	1.142	0.944	0.0017	0.0017	55.4	116.7	153.7	351.8
62	294.0	52.5	84.4	59.6	1.160	0.804	0.311	0.0040	71.6	156.0	168.1	61.8	0.0017	0.366	0.0055	64.9	1.142	0.787	0.0040	0.0040	70.7	129.1	166.1	309.9
63	87.5	32.4	24.3	23.2	1.190	0.784	0.130	0.0018	58.6	83.0	90.6	38.2	0.0067	0.278	0.0039	25.2	1.171	0.765	0.0015	0.0015	49.5	60.7	83.6	100.7
64	95.0	32.4	24.3	23.2	1.190	0.784	0.130	0.0018	58.6	83.0	90.6	38.2	0.0067	0.278	0.0039	25.2	1.171	0.765	0.0015	0.0015	49.5	60.7	83.6	100.7
65	94.0	32.4	24.3	23.2	1.190	0.784	0.130	0.0018	55.3	79.6	88.2	38.2	0.0044	0.314	0.0044	25.2	1.171	0.765	0.0015	0.0015	46.6	58.4	81.3	72.0
66	99.5	32.4	24.3	23.2	1.190	0.784	0.130	0.0018	55.3	79.6	88.2	38.2	0.0044	0.314	0.0044	25.2	1.171	0.765	0.0015	0.0015	46.6	58.4	81.3	72.0
67	242.0	46.2	100.7	///	///	///	///	0.0040	12.8	113.5	135.2	54.4	0.0008	///	///	///	///	///	0.0040	0.0040	12.8	93.8	126.4	265.3
68	270.0	46.2	100.7	///	///	///	///	0.0040	25.6	126.3	145.6	54.4	0.0016	///	///	///	///	///	0.0040	0.0040	25.6	102.0	134.6	275.5
69	318.0	46.2	100.7	///	///	///	///	0.0040	38.4	139.1	155.9	54.4	0.0024	///	///	///	///	///	0.0040	0.0040	38.4	110.2	142.8	286.1
70	279.0	46.2	100.7	///	///	///	///	0.0040	38.4	139.1	155.9	54.4	0.0024	///	///	///	///	///	0.0040	0.0040	38.4	110.2	142.8	286.1
71	105.9	39.0	0.0	64.8	1.124	0.568	0.235	0.0035	26.6	26.6	52.4	45.9	0.0007	0.465	0.0069	70.5	1.107	0.530	0.0028	0.0028	21.5	17.4	45.0	116.4
72	127.9	39.0	0.0	///	///	///	///	0.0040	30.6	30.6	57.9	45.9	0.0007	///	///	///	///	///	0.0040	0.0040	30.6	24.8	52.4	133.8
73	105.4	39.0	0.0	64.8	1.124	0.784	0.324	0.0040	30.6	30.6	55.3	45.9	0.0007	0.465	0.0069	70.5	1.107	0.765	0.0040	0.0040	30.6	24.8	52.4	130.4
74	123.8	39.0	0.0	64.8	1.124	0.568	0.235	0.0035	53.3	53.3	71.7	45.9	0.0015	0.377	0.0056	70.5	1.107	0.530	0.0028	0.0028	43.0	34.8	62.4	128.3

No.																							
75	125.4	39.0	0.0	64.8	1.124	0.784	0.324	0.0048	73.5	73.5	86.3	45.9	0.0015	0.377	0.0056	70.5	1.107	0.765	0.0040	0.0040	61.3	49.6	77.2	149.6
76	193.2	39.0	0.0	///	///	///	///	0.0040	61.3	61.3	82.7	45.9	0.0015	0.377	0.0056	70.5	1.107	#VALUE!	0.0040	0.0040	61.3	49.6	77.2	158.5
77	124.5	39.0	0.0	64.8	1.124	0.568	0.235	0.0035	75.3	75.3	87.6	45.9	0.0015	0.377	0.0056	70.5	1.107	0.530	0.0028	0.0028	60.7	49.2	76.8	128.3
78	127.7	39.0	0.0	15.9	1.124	0.894	0.110	0.0013	115.7	115.7	116.8	45.9	0.0093	0.225	0.0027	17.3	1.107	0.885	0.0011	0.0011	99.0	80.2	107.7	132.0
79	130.7	39.0	0.0	15.9	1.124	0.894	0.110	0.0013	115.7	115.7	116.8	45.9	0.0066	0.249	0.0030	17.3	1.107	0.885	0.0011	0.0011	99.0	80.2	107.7	125.6
80	153.9	49.1	0.0	33.5	1.493	0.554	0.158	0.0023	55.6	55.6	81.9	57.8	0.0045	0.292	0.0043	36.4	1.469	0.515	0.0019	0.0019	44.7	36.2	70.9	123.2
81	153.9	48.7	0.0	33.5	1.476	0.777	0.219	0.0032	77.1	77.1	97.1	57.3	0.0023	0.358	0.0053	36.4	1.453	0.757	0.0027	0.0027	65.0	52.6	87.0	145.0
82	134.7	49.1	0.0	33.5	1.493	0.554	0.158	0.0023	27.8	27.8	61.9	57.8	0.0023	0.359	0.0053	36.4	1.469	0.515	0.0019	0.0019	22.3	18.1	52.8	135.2
83	187.6	48.9	0.0	33.5	1.483	0.777	0.220	0.0032	155.0	155.0	153.5	57.5	0.0045	0.291	0.0043	36.4	1.460	0.757	0.0027	0.0027	130.5	105.7	140.2	169.9
84	134.7	49.5	0.0	33.5	1.507	0.777	0.224	0.0033	39.4	39.4	70.5	58.2	0.0011	0.444	0.0065	36.4	1.483	0.757	0.0028	0.0028	33.2	26.9	61.8	131.4
85	139.5	49.1	0.0	33.5	1.490	0.554	0.158	0.0023	27.8	27.8	61.8	57.7	0.0023	0.359	0.0053	36.4	1.467	0.515	0.0019	0.0019	22.3	18.1	52.7	135.2
86	139.5	48.5	0.0	33.5	1.469	0.777	0.218	0.0032	38.4	38.4	69.0	57.1	0.0011	0.440	0.0065	36.4	1.446	0.757	0.0027	0.0027	32.3	26.2	60.5	129.7
87	168.3	49.8	0.0	33.5	1.518	0.777	0.226	0.0033	79.3	79.3	99.6	58.5	0.0023	0.361	0.0053	36.4	1.494	0.757	0.0028	0.0028	66.8	54.1	89.2	146.9
88	129.9	50.3	0.0	33.5	1.539	0.554	0.163	0.0024	14.3	14.3	53.1	59.1	0.0011	0.447	0.0066	36.4	1.515	0.515	0.0019	0.0019	11.5	9.3	44.8	118.9
89	129.9	49.3	0.0	33.5	1.499	0.777	0.223	0.0033	19.6	19.6	56.0	58.0	0.0006	0.545	0.0080	36.4	1.475	0.757	0.0028	0.0028	16.5	13.4	48.1	119.7
90	125.0	48.8	0.0	33.5	1.479	0.554	0.157	0.0023	13.8	13.8	51.4	57.4	0.0011	0.441	0.0065	36.4	1.455	0.515	0.0018	0.0018	11.1	9.0	43.4	119.3
91	155.0	53.9	0.0	51.7	1.190	0.816	0.254	0.0040	84.7	84.7	107.0	63.4	0.0022	0.342	0.0057	56.3	1.171	0.800	0.0036	0.0036	75.7	61.3	99.4	151.1
92	157.5	53.9	0.0	34.6	1.190	0.850	0.177	0.0029	92.7	92.7	112.8	63.4	0.0044	0.278	0.0046	37.6	1.171	0.836	0.0025	0.0025	78.1	63.2	101.3	142.4
93	162.0	53.9	0.0	51.7	1.190	0.816	0.254	0.0040	33.9	33.9	70.3	63.4	0.0009	0.450	0.0075	56.3	1.171	0.800	0.0036	0.0036	30.3	24.5	62.6	105.0
94	121.5	53.9	0.0	51.7	1.190	0.550	0.171	0.0028	19.7	19.7	60.0	63.4	0.0009	0.450	0.0075	56.3	1.171	0.511	0.0023	0.0023	15.8	12.8	50.8	110.1
95	221.0	53.9	0.0	51.7	1.190	0.849	0.265	0.0040	103.2	103.2	120.4	63.4	0.0022	0.342	0.0057	56.3	1.171	0.836	0.0037	0.0037	96.4	78.1	116.1	177.4
96	177.0	28.3	133.5	34.6	0.799	0.876	0.123	0.0020	79.7	213.2	117.6	33.3	0.0044	0.246	0.0041	37.6	0.786	0.866	0.0017	0.0017	67.5	167.9	100.0	226.5
97	180.5	28.3	133.5	34.6	0.799	0.876	0.123	0.0020	79.7	213.2	117.6	33.3	0.0044	0.246	0.0041	37.6	0.786	0.866	0.0017	0.0017	67.5	167.9	100.0	226.5
98	131.0	33.9	0.0	51.7	1.012	0.830	0.220	0.0037	33.5	33.5	53.0	39.9	0.0009	0.429	0.0071	56.3	0.996	0.816	0.0031	0.0031	28.5	23.1	47.0	117.9
99	133.5	33.9	0.0	51.7	1.012	0.830	0.220	0.0037	50.3	50.3	65.2	39.9	0.0013	0.379	0.0063	56.3	0.996	0.816	0.0031	0.0031	42.7	34.6	58.5	123.5
100	144.5	33.9	0.0	51.7	1.012	0.830	0.220	0.0037	83.8	83.8	89.4	39.9	0.0022	0.326	0.0054	56.3	0.996	0.816	0.0031	0.0031	71.2	57.6	81.6	143.2
101	155.0	34.1	0.0	51.7	1.012	0.830	0.220	0.0037	83.8	83.8	89.6	40.1	0.0022	0.326	0.0054	56.3	0.996	0.816	0.0031	0.0031	71.2	57.6	81.7	143.2
102	169.5	33.9	0.0	34.6	1.012	0.773	0.137	0.0023	112.1	112.1	109.8	39.9	0.0044	0.264	0.0044	37.6	0.996	0.877	0.0022	0.0022	90.3	73.2	97.1	150.9
103	127.5	34.1	0.0	51.7	1.012	0.830	0.220	0.0037	33.5	33.5	53.2	40.1	0.0009	0.429	0.0071	56.3	0.996	0.816	0.0031	0.0031	28.5	23.1	47.1	117.6
104	214.0	33.8	111.2	34.6	1.012	0.773	0.148	0.0023	112.1	223.3	140.4	39.8	0.0044	0.264	0.0041	37.6	0.996	0.753	0.0019	0.0019	95.1	171.4	119.4	182.7
105	131.0	45.6	0.0	34.6	1.511	0.773	0.221	0.0034	137.8	137.8	138.4	53.7	0.0044	0.298	0.0046	37.6	1.487	0.753	0.0029	0.0029	116.8	94.6	126.8	166.4
106	88.0	29.2	0.0	51.7	0.831	0.830	0.195	0.0030	27.5	27.5	44.7	34.4	0.0009	0.404	0.0062	56.3	0.818	0.816	0.0025	0.0025	23.4	18.9	39.6	107.4
107	113.0	29.2	0.0	51.7	0.831	0.830	0.195	0.0030	68.9	68.9	74.6	34.4	0.0012	0.307	0.0047	56.3	0.818	0.816	0.0025	0.0025	58.4	47.3	68.0	131.7
108	119.0	45.6	0.0	51.7	1.511	0.830	0.354	0.0040	91.8	91.8	105.1	53.7	0.0022	0.367	0.0057	56.3	1.487	0.816	0.0040	0.0040	91.8	74.4	106.6	155.7
109	140.0	45.6	0.0	///	///	///	///	0.0040	91.8	91.8	112.9	53.7	0.0022	///	///	///	///	///	0.0040	0.0040	91.8	74.4	106.6	150.0
110	91.2	43.0	0.0	///	///	///	///	0.0040	7.7	7.7	42.8	50.6	0.0006	///	///	///	///	///	0.0040	0.0040	7.7	5.6	35.9	125.9
111	89.7	45.5	0.0	///	///	///	///	0.0040	3.9	3.9	41.8	53.5	0.0003	///	///	///	///	///	0.0040	0.0040	3.9	2.8	34.9	104.8
112	114.0	46.4	0.0	///	///	///	///	0.0040	15.4	15.4	51.9	54.6	0.0012	///	///	///	///	///	0.0040	0.0040	15.4	11.1	43.9	134.3
113	214.0	83.4	0.0	///	///	///	///	0.0040	65.0	65.0	123.4	98.1	0.0007	///	///	///	///	///	0.0040	0.0040	65.0	52.7	111.5	232.1
114	159.0	83.4	0.0	///	///	///	///	0.0040	32.5	32.5	97.1	98.1	0.0004	///	///	///	///	///	0.0040	0.0040	32.5	26.3	85.2	182.9
115	116.0	46.4	0.0	///	///	///	///	0.0040	32.5	32.5	65.7	54.6	0.0007	///	///	///	///	///	0.0040	0.0040	32.5	26.3	59.1	126.7
116	110.0	41.8	0.0	///	///	///	///	0.0040	7.7	7.7	41.7	49.1	0.0006	///	///	///	///	///	0.0040	0.0040	7.7	5.6	35.1	124.1

No.	V_{U-exp}	V_c	V_s	L_e	K_1	K_2	K_v	ε_{fe}	V_f	Check Equation (17)	$\emptyset V_{n-ACI}$	V_c	ρ_{frp}	R	ε_{frpe-1}	L_e	K_1	K_2	ε_{frpe-2}	Min. ε_{frpe}	V_{frp}	Check Equation (30)	V_{r-ABA}	V_{ANN}
117	173.0	88.9	0.0	///	///	///	///	0.0040	7.7	7.7	81.7	104.5	0.0003	///	///	///	///	///	0.0040	0.0040	7.7	5.6	68.3	221.7
118	209.0	83.5	0.0	///	///	///	///	0.0040	15.4	15.4	83.4	98.3	0.0006	///	///	///	///	///	0.0040	0.0040	15.4	11.1	70.1	222.0
119	224.0	88.8	0.0	///	///	///	///	0.0040	15.4	15.4	87.9	104.5	0.0006	///	///	///	///	///	0.0040	0.0040	15.4	11.1	73.8	222.6
120	254.0	84.3	0.0	///	///	///	///	0.0040	25.2	25.2	92.0	99.2	0.0010	///	///	///	///	///	0.0040	0.0040	25.2	18.2	77.8	223.8
121	247.0	84.7	0.0	///	///	///	///	0.0040	37.8	37.8	102.6	99.7	0.0014	///	///	///	///	///	0.0040	0.0040	37.8	27.4	87.2	226.2
122	240.0	85.1	0.0	///	///	///	///	0.0040	50.5	50.5	113.1	100.1	0.0019	///	///	///	///	///	0.0040	0.0040	50.5	36.5	96.6	228.7
123	424.0	170.2	0.0	///	///	///	///	0.0040	25.2	25.2	165.0	200.2	0.0005	///	///	///	///	///	0.0040	0.0040	25.2	18.2	138.4	423.3
124	379.0	192.8	0.0	///	///	///	///	0.0040	37.8	37.8	194.4	226.8	0.0006	///	///	///	///	///	0.0040	0.0040	37.8	27.4	163.5	379.3
125	569.0	294.7	0.0	///	///	///	///	0.0040	46.3	46.3	287.9	346.7	0.0005	///	///	///	///	///	0.0040	0.0040	46.3	33.4	241.5	658.3
126	662.0	297.3	0.0	///	///	///	///	0.0040	92.5	92.5	327.4	349.7	0.0010	///	///	///	///	///	0.0040	0.0040	92.5	66.9	276.7	660.8
127	209.1	97.1	0.0	///	///	///	///	0.0040	42.9	42.9	117.2	114.2	0.0004	///	///	///	///	///	0.0040	0.0040	42.9	34.8	103.3	189.8
128	218.6	97.1	0.0	///	///	///	///	0.0040	24.3	24.3	102.2	114.2	0.0005	///	///	///	///	///	0.0040	0.0040	24.3	17.6	86.1	160.7
129	469.7	240.0	0.0	///	///	///	///	0.0040	96.2	96.2	281.7	282.3	0.0004	///	///	///	///	///	0.0040	0.0040	96.2	77.9	247.3	506.1
130	464.5	240.0	0.0	///	///	///	///	0.0040	54.5	54.5	248.0	282.3	0.0005	///	///	///	///	///	0.0040	0.0040	54.5	39.4	208.8	468.1
131	73.7	33.4	0.0	17.3	1.383	0.848	0.090	0.0017	61.0	61.0	72.5	39.3	0.0062	0.125	0.0024	18.9	1.362	0.835	0.0011	0.0011	40.9	26.1	49.8	73.7
132	63.9	33.4	0.0	17.3	1.383	0.848	0.090	0.0017	61.0	61.0	72.5	39.3	0.0062	0.125	0.0024	18.9	1.362	0.835	0.0011	0.0011	40.9	26.1	49.8	73.7
133	82.2	33.4	0.0	17.3	1.383	0.848	0.090	0.0017	86.2	86.2	90.7	39.3	0.0062	0.125	0.0024	18.9	1.362	0.835	0.0011	0.0011	57.9	36.9	60.7	73.7
134	55.7	33.4	0.0	17.3	1.383	0.848	0.090	0.0017	86.2	86.2	90.7	39.3	0.0062	0.125	0.0024	18.9	1.362	0.835	0.0011	0.0011	57.9	36.9	60.7	73.7
135	53.6	33.4	0.0	66.9	1.383	0.415	0.242	0.0032	35.6	35.6	54.1	39.3	0.0043	0.410	0.0055	72.8	1.362	0.363	0.0024	0.0024	26.9	21.8	45.4	92.6
136	51.2	33.4	0.0	66.9	1.383	0.415	0.242	0.0032	35.6	35.6	54.1	39.3	0.0043	0.410	0.0055	72.8	1.362	0.363	0.0024	0.0024	26.9	21.8	45.4	92.6
137	84.6	23.0	0.0	19.7	1.356	0.828	0.098	0.0019	66.4	66.4	67.5	27.0	0.0093	0.102	0.0019	21.5	1.334	0.812	0.0012	0.0012	44.5	28.4	44.7	107.1
138	104.6	23.0	0.0	19.7	1.356	0.828	0.098	0.0019	66.4	66.4	67.5	27.0	0.0093	0.102	0.0019	21.5	1.334	0.812	0.0012	0.0012	44.5	28.4	44.7	107.1
139	97.0	23.0	0.0	19.7	1.356	0.828	0.098	0.0019	94.0	94.0	95.3	27.0	0.0093	0.102	0.0019	21.5	1.334	0.812	0.0012	0.0012	62.9	40.1	56.5	107.1
140	121.5	23.0	0.0	19.7	1.356	0.828	0.098	0.0019	94.0	94.0	95.3	27.0	0.0093	0.102	0.0019	21.5	1.334	0.812	0.0012	0.0012	62.9	40.1	56.5	107.1
141	76.5	23.0	0.0	66.9	1.356	0.416	0.238	0.0032	35.0	35.0	44.8	27.0	0.0065	0.362	0.0048	72.8	1.335	0.364	0.0024	0.0024	26.5	21.5	37.7	85.9
142	128.6	23.0	0.0	66.9	1.356	0.416	0.238	0.0032	35.0	35.0	44.8	27.0	0.0065	0.362	0.0048	72.8	1.335	0.364	0.0024	0.0024	26.5	21.5	37.7	85.9
143	87.7	23.0	0.0	44.8	1.356	0.609	0.234	0.0031	68.7	68.7	69.1	27.0	0.0129	0.294	0.0039	48.7	1.335	0.575	0.0025	0.0025	56.0	45.3	61.6	93.3
144	133.5	23.0	0.0	44.8	1.356	0.609	0.234	0.0031	68.7	68.7	69.1	27.0	0.0129	0.294	0.0039	48.7	1.335	0.575	0.0025	0.0025	56.0	45.3	61.6	93.3
145	96.1	23.0	0.0	66.9	1.356	0.708	0.406	0.0040	44.2	44.2	51.4	27.0	0.0065	0.362	0.0048	72.8	1.335	0.682	0.0040	0.0040	44.2	35.8	52.0	90.9
146	126.8	23.0	0.0	66.9	1.356	0.708	0.406	0.0040	44.2	44.2	51.4	27.0	0.0065	0.362	0.0048	72.8	1.335	0.682	0.0040	0.0040	44.2	35.8	52.0	90.9
147	63.6	25.8	0.0	34.2	1.199	0.544	0.125	0.0019	43.2	43.2	53.1	30.3	0.0045	0.276	0.0041	37.2	1.180	0.504	0.0015	0.0015	34.6	27.9	46.2	65.7
148	58.6	25.1	0.0	51.1	1.155	0.319	0.105	0.0016	18.2	18.2	34.5	29.5	0.0022	0.337	0.0050	55.6	1.137	0.259	0.0011	0.0011	12.8	10.3	28.1	75.0
149	60.3	24.3	0.0	34.2	1.109	0.544	0.116	0.0017	39.9	39.9	49.5	28.6	0.0045	0.270	0.0041	37.2	1.091	0.504	0.0014	0.0014	32.0	25.8	43.1	67.1
150	80.8	24.1	0.0	34.2	1.097	0.658	0.138	0.0021	63.7	63.7	66.6	28.4	0.0045	0.269	0.0040	37.2	1.080	0.628	0.0017	0.0017	52.6	42.4	59.6	78.7
151	68.5	25.2	0.0	51.1	1.160	0.659	0.219	0.0033	37.8	37.8	48.7	29.6	0.0022	0.337	0.0051	55.6	1.142	0.629	0.0027	0.0027	31.2	25.2	43.1	71.3
152	85.8	25.4	0.0	51.1	1.176	0.745	0.251	0.0038	57.8	57.8	63.3	29.9	0.0022	0.338	0.0051	55.6	1.158	0.722	0.0032	0.0032	48.4	39.1	57.2	87.9
153	132.1	43.9	0.0	///	///	///	///	0.0040	28.1	28.1	57.6	51.6	///	///	///	///	///	///	0.0040	0.0040	28.1	22.7	53.7	118.5
154	180.9	42.2	31.9	///	///	///	///	0.0040	28.1	60.0	83.3	49.7	///	///	///	///	///	///	0.0040	0.0040	28.1	49.8	79.7	199.4
155	213.8	39.4	71.6	///	///	///	///	0.0040	28.1	99.6	114.6	46.4	///	///	///	///	///	///	0.0040	0.0040	28.1	83.5	111.4	221.5
156	55.5	28.5	0.0	20.5	1.430	0.795	0.043	0.0020	58.2	58.2	66.3	33.6	0.0064	0.294	0.0132	22.3	1.407	0.777	0.0017	0.0017	49.2	39.7	60.0	64.4

157	55.0	30.8	0.0	20.5	1.583	0.488	0.030	0.0013	39.6	39.6	54.8	36.2	0.0160	0.230	0.0104	22.3	1.558	0.443	0.0010	0.0010	31.0	25.1	31.0	46.9	13.0
158	58.0	30.2	0.0	20.5	1.542	0.795	0.047	0.0021	74.0	74.0	79.1	35.5	0.0053	0.318	0.0143	22.3	1.518	0.777	0.0018	0.0018	62.5	50.5	62.5	71.9	62.7
159	65.0	30.2	0.0	20.5	1.539	0.795	0.047	0.0021	65.2	65.2	72.8	35.5	0.0053	0.318	0.0143	22.3	1.515	0.777	0.0018	0.0018	55.1	44.5	55.1	65.9	62.6
160	99.7	29.3	0.0	20.5	1.480	0.795	0.045	0.0020	150.6	150.6	121.5	34.5	0.0160	0.226	0.0102	22.3	1.456	0.777	0.0017	0.0017	127.2	102.7	127.2	103.4	92.5
161	85.0	31.4	0.0	20.5	1.622	0.795	0.049	0.0022	165.0	165.0	130.2	36.9	0.0160	0.232	0.0104	22.3	1.596	0.777	0.0019	0.0019	139.4	112.6	139.4	110.7	92.6
162	97.5	28.6	0.0	20.5	1.435	0.795	0.044	0.0020	146.1	146.1	118.8	33.7	0.0160	0.224	0.0101	22.3	1.413	0.777	0.0017	0.0017	123.4	99.6	123.4	101.1	92.3
163	94.0	26.9	0.0	20.5	1.319	0.795	0.040	0.0018	189.8	189.8	111.5	31.6	0.0160	0.218	0.0098	22.3	1.298	0.777	0.0015	0.0015	160.3	129.4	160.3	94.9	90.4
164	86.9	30.1	0.0	38.7	1.536	0.807	0.089	0.0040	99.4	99.4	97.4	35.4	0.0036	0.317	0.0143	42.1	1.512	0.790	0.0034	0.0034	84.6	68.3	84.6	89.8	60.6
165	80.0	29.9	0.0	25.9	1.524	0.871	0.064	0.0029	143.3	143.3	124.2	35.2	0.0072	0.257	0.0116	28.1	1.500	0.859	0.0025	0.0025	122.2	98.7	122.2	105.7	67.8
166	95.7	13.8	26.6	87.3	0.924	0.444	0.190	0.0030	41.0	14.4	44.8	16.3	0.0014	0.362	0.0057	95.0	0.910	0.395	0.0023	0.0023	11.1	31.6	11.1	41.4	94.6
167	105.1	13.8	26.6	58.4	0.924	0.628	0.180	0.0028	53.9	27.3	57.5	16.3	0.0028	0.294	0.0046	63.6	0.910	0.595	0.0023	0.0023	22.3	40.6	22.3	48.9	92.6
168	68.5	13.8	0.0	58.4	0.924	0.628	0.180	0.0028	27.3	27.3	31.5	16.3	0.0028	0.294	0.0046	63.6	0.910	0.595	0.0023	0.0023	22.3	18.0	22.3	27.9	74.2
169	59.3	13.8	0.0	87.3	0.924	0.444	0.190	0.0030	14.4	14.4	22.2	16.3	0.0014	0.362	0.0057	95.0	0.910	0.395	0.0023	0.0023	11.1	8.9	11.1	18.7	76.1
170	247.0	107.7	0.0	83.8	1.838	0.665	0.453	0.0040	92.6	92.6	158.5	126.7	0.0008	0.528	0.0100	91.1	1.809	0.635	0.0040	0.0040	92.6	74.8	92.6	151.1	278.9
171	257.0	110.9	0.0	64.4	1.911	0.742	0.404	0.0040	145.6	145.6	199.4	130.4	0.0012	0.466	0.0089	70.1	1.881	0.720	0.0040	0.0040	145.6	117.6	145.6	196.2	284.0
172	305.0	95.8	0.0	64.4	1.571	0.742	0.332	0.0040	145.6	145.6	186.6	112.7	0.0012	0.440	0.0084	70.1	1.546	0.720	0.0040	0.0040	145.6	117.6	145.6	185.5	247.1
173	338.0	89.2	0.0	///	///	///	///	0.0040	130.7	130.7	181.4	105.0	///	///	///	///	///	///	0.0040	0.0040	130.7	105.5	130.7	168.8	359.9
174	306.0	107.7	0.0	64.4	1.838	0.742	0.389	0.0040	145.6	145.6	196.7	126.7	0.0012	0.461	0.0088	70.1	1.809	0.720	0.0040	0.0040	145.6	117.6	145.6	193.9	279.2
175	251.0	90.2	0.0	64.4	1.450	0.742	0.307	0.0040	145.6	145.6	181.9	106.1	0.0012	0.429	0.0082	70.1	1.427	0.720	0.0040	0.0040	145.6	117.6	145.6	181.6	226.5
176	256.0	101.1	0.0	64.4	1.688	0.742	0.357	0.0040	103.0	103.0	160.3	118.9	0.0012	0.449	0.0085	70.1	1.662	0.720	0.0040	0.0040	103.0	83.1	103.0	154.7	263.8
177	298.0	94.9	0.0	64.4	1.551	0.742	0.328	0.0040	103.0	103.0	155.0	111.6	0.0012	0.438	0.0083	70.1	1.527	0.720	0.0040	0.0040	103.0	83.1	103.0	150.4	243.9
178	367.0	94.9	0.0	///	///	///	///	0.0040	103.0	103.0	163.8	111.6	///	///	///	///	///	///	0.0040	0.0040	103.0	83.1	103.0	150.4	361.4
179	388.0	89.2	0.0	///	///	///	///	0.0040	92.4	92.4	150.5	105.0	///	///	///	///	///	///	0.0040	0.0040	92.4	74.6	92.4	137.8	359.9
180	334.0	110.9	0.0	50.9	1.911	0.796	0.343	0.0040	218.4	218.4	270.6	130.4	0.0018	0.413	0.0078	55.4	1.881	0.778	0.0040	0.0040	218.4	176.3	218.4	255.1	283.9
181	298.0	69.5	39.6	50.9	1.429	0.745	0.240	0.0040	163.1	123.6	182.0	81.8	0.0018	0.378	0.0072	55.4	1.406	0.723	0.0038	0.0038	118.0	129.0	118.0	178.3	299.8
182	298.0	69.5	39.6	50.9	1.429	0.745	0.240	0.0040	163.1	123.6	182.0	81.8	0.0018	0.378	0.0072	55.4	1.406	0.723	0.0038	0.0038	118.0	129.0	118.0	178.3	299.8
183	250.0	80.0	43.4	///	///	///	///	0.0040	312.9	269.5	332.2	94.2	///	///	///	///	///	///	0.0040	0.0040	269.5	254.5	269.5	282.5	284.2
184	330.0	80.0	57.8	///	///	///	///	0.0040	327.4	269.5	332.2	94.2	///	///	///	///	///	///	0.0040	0.0040	269.5	266.8	269.5	282.5	296.6
185	300.0	80.0	86.8	///	///	///	///	0.0040	356.3	269.5	332.2	94.2	///	///	///	///	///	///	0.0040	0.0040	269.5	291.4	269.5	282.5	322.3
186	270.0	80.0	57.8	34.7	0.845	0.923	0.379	0.0023	211.1	153.2	227.9	94.2	0.0015	0.292	0.0018	37.7	0.832	0.916	0.0020	0.0020	131.4	155.3	131.4	212.1	252.7
187	280.0	80.0	86.8	34.7	0.845	0.923	0.379	0.0023	240.0	153.2	252.5	94.2	0.0015	0.292	0.0018	37.7	0.832	0.916	0.0020	0.0020	131.4	179.9	131.4	236.7	278.2
188	225.0	80.0	43.4	34.7	0.845	0.923	0.379	0.0023	196.6	153.2	215.6	94.2	0.0015	0.292	0.0018	37.7	0.832	0.916	0.0020	0.0020	131.4	143.0	131.4	199.8	241.0
189	205.0	80.0	57.8	34.7	0.845	0.846	0.347	0.0021	198.3	140.4	218.7	94.2	0.0015	0.292	0.0018	37.7	0.832	0.832	0.0018	0.0018	119.4	145.6	119.4	202.4	213.2
190	240.0	80.0	86.8	34.7	0.845	0.846	0.347	0.0021	227.2	140.4	243.2	94.2	0.0015	0.292	0.0018	37.7	0.832	0.832	0.0018	0.0018	119.4	170.2	119.4	227.0	231.2
191	180.0	80.0	43.4	34.7	0.845	0.846	0.347	0.0021	183.8	140.4	206.4	94.2	0.0015	0.292	0.0018	37.7	0.832	0.832	0.0018	0.0018	119.4	133.3	119.4	190.1	206.1
192	220.0	80.0	57.8	34.7	0.845	0.846	0.347	0.0021	198.3	140.4	218.7	94.2	0.0015	0.292	0.0018	37.7	0.832	0.832	0.0018	0.0018	119.4	145.6	119.4	202.4	213.2
193	120.0	33.4	0.0	51.0	1.012	0.660	0.191	0.0029	66.2	66.2	76.3	39.3	0.0022	0.323	0.0048	55.5	0.996	0.630	0.0024	0.0024	54.6	44.1	54.6	67.9	116.3
194	112.8	33.4	0.0	27.0	1.012	0.820	0.099	0.0019	130.5	130.5	138.7	39.3	0.0066	0.232	0.0044	29.3	0.996	0.804	0.0016	0.0016	110.6	89.3	110.6	113.2	124.3
195	140.2	33.4	0.0	27.0	1.012	0.820	0.099	0.0019	130.5	130.5	138.7	39.3	0.0066	0.232	0.0044	29.3	0.996	0.804	0.0016	0.0016	110.6	89.3	110.6	113.2	124.3
196	193.0	35.7	52.8	34.1	1.106	0.773	0.129	0.0025	166.1	113.3	148.2	42.0	0.0044	0.270	0.0051	37.1	1.089	0.753	0.0021	0.0021	113.3	121.9	95.4	126.1	206.7
197	213.3	35.7	52.8	27.0	1.106	0.820	0.108	0.0021	195.4	142.7	148.2	42.0	0.0066	0.239	0.0045	29.3	1.089	0.804	0.0017	0.0017	120.9	142.5	120.9	126.1	207.0
198	247.5	35.7	52.8	27.0	1.106	0.820	0.108	0.0021	195.4	142.7	148.2	42.0	0.0066	0.239	0.0045	29.3	1.089	0.804	0.0017	0.0017	120.9	142.5	120.9	126.1	207.0

No.	V_{U-exp}	V_c	V_s	L_e	K_1	K_2	K_v	ε_{je}	V_f	Check Equation (17)	$øV_{n-ACI}$	V_c	ρ_{frp}	R	ε_{frpe-1}	L_e	K_1	K_2	ε_{frpe-2}	Min. ε_{frpe}	V_{frp}	Check Equation (30)	V_{n-ABA}	V_{ANN}
199	161.4	35.7	52.8	51.0	1.106	0.660	0.165	0.0031	72.4	125.2	127.5	42.0	0.0022	0.332	0.0063	55.5	1.089	0.630	0.0026	0.0026	59.7	93.1	118.4	206.6
200	208.8	35.7	52.8	34.1	1.106	0.773	0.129	0.0025	113.3	166.1	148.2	42.0	0.0044	0.270	0.0051	37.1	1.089	0.753	0.0021	0.0021	95.4	121.9	126.1	206.7
201	212.0	35.7	52.8	34.1	1.106	0.773	0.129	0.0025	113.3	166.1	148.2	42.0	0.0044	0.270	0.0051	37.1	1.089	0.753	0.0021	0.0021	95.4	121.9	126.1	206.7
202	252.9	43.3	75.4	51.5	1.433	0.828	0.342	0.0040	91.1	166.5	166.7	51.0	0.0022	0.360	0.0054	56.0	1.411	0.813	0.0040	0.0040	91.1	137.6	152.9	256.5
203	264.8	43.3	75.4	34.4	1.433	0.885	0.245	0.0037	167.1	242.5	179.8	51.0	0.0044	0.293	0.0044	37.4	1.411	0.875	0.0031	0.0031	142.8	179.4	152.9	260.3
204	238.9	43.3	62.1	51.5	1.433	0.828	0.342	0.0040	91.1	153.2	155.4	51.0	0.0022	0.360	0.0054	56.0	1.411	0.813	0.0040	0.0040	91.1	126.3	152.9	244.7
205	243.3	43.3	62.1	34.4	1.433	0.885	0.245	0.0037	167.1	229.2	179.8	51.0	0.0044	0.293	0.0044	37.4	1.411	0.875	0.0031	0.0031	142.8	168.1	152.9	249.5
206	142.5	57.9	19.2	46.5	1.257	0.897	0.331	0.0040	32.5	51.7	89.0	68.1	0.0013	0.511	0.0068	50.6	1.237	0.888	0.0038	0.0038	30.6	41.1	82.0	144.8
207	130.0	57.9	19.2	46.5	1.257	0.897	0.331	0.0040	26.0	45.2	84.3	68.1	0.0011	0.546	0.0073	50.6	1.237	0.888	0.0038	0.0038	24.5	36.1	77.1	142.8
208	154.5	57.9	19.2	46.5	1.257	0.897	0.331	0.0040	30.6	49.9	87.7	68.1	0.0009	0.577	0.0077	50.6	1.237	0.888	0.0038	0.0038	28.9	39.7	80.6	141.5
209	150.0	57.9	19.2	46.5	1.257	0.897	0.331	0.0040	26.3	45.5	84.5	68.1	0.0008	0.604	0.0080	50.6	1.237	0.888	0.0038	0.0038	24.8	36.3	77.3	140.6
210	177.5	57.9	19.2	///	///	///	///	0.0040	32.5	51.7	91.8	68.1	///	///	///	///	///	///	0.0040	0.0040	32.5	42.6	83.5	153.9
211	155.0	57.9	19.2	///	///	///	///	0.0040	26.0	45.2	86.6	68.1	///	///	///	///	///	///	0.0040	0.0040	26.0	37.3	78.3	149.8
212	145.5	57.9	19.2	///	///	///	///	0.0040	30.6	49.9	90.3	68.1	///	///	///	///	///	///	0.0040	0.0040	30.6	41.1	82.0	147.3
213	132.0	57.9	19.2	///	///	///	///	0.0040	26.3	45.5	86.8	68.1	///	///	///	///	///	///	0.0040	0.0040	26.3	37.6	78.5	145.7
214	110.0	41.9	15.1	66.6	1.707	0.697	0.536	0.0040	14.3	29.3	58.7	49.3	0.0006	0.565	0.0070	72.5	1.680	0.671	0.0040	0.0040	14.3	24.3	53.9	127.9
215	152.5	41.5	15.1	53.1	1.688	0.759	0.461	0.0040	25.3	40.4	66.4	48.9	0.0011	0.474	0.0059	57.7	1.662	0.738	0.0040	0.0040	25.3	33.3	62.6	135.6
216	121.5	41.9	15.1	64.3	1.707	0.708	0.435	0.0040	13.0	28.1	57.8	49.3	0.0005	0.580	0.0087	69.9	1.680	0.682	0.0040	0.0040	13.0	23.3	52.9	121.6
217	137.5	40.8	15.1	64.3	1.650	0.708	0.421	0.0040	13.0	28.1	56.9	48.0	0.0005	0.574	0.0086	69.9	1.624	0.682	0.0040	0.0040	13.0	23.3	52.2	120.1
218	103.5	40.1	15.1	12.5	1.611	0.886	0.375	0.0015	95.6	110.7	116.0	47.2	0.0078	0.234	0.0009	13.6	1.585	0.876	0.0013	0.0009	59.5	60.8	89.3	101.8
219	701.0	90.3	76.0	34.4	1.253	0.957	0.231	0.0035	421.1	497.2	374.8	106.2	0.0055	0.263	0.0039	37.4	1.233	0.953	0.0030	0.0030	362.5	357.3	318.7	700.9
220	71.1	21.8	19.3	36.6	1.224	0.820	0.270	0.0031	85.5	104.7	90.4	25.6	0.0315	0.274	0.0031	39.8	1.204	0.804	0.0026	0.0026	72.4	74.9	76.9	85.3
221	71.6	21.8	19.3	37.1	1.224	0.817	0.263	0.0031	84.5	103.8	90.4	25.6	0.0315	0.276	0.0033	40.3	1.204	0.801	0.0026	0.0026	71.6	74.2	76.9	85.6
222	97.0	21.8	19.3	48.2	1.224	0.525	0.300	0.0026	63.4	82.7	80.7	25.6	0.0236	0.316	0.0027	52.5	1.204	0.483	0.0021	0.0021	50.5	57.1	72.6	70.7
223	62.0	24.1	13.9	57.7	0.594	0.798	0.127	0.0023	6.8	20.7	37.3	28.4	0.0004	0.470	0.0085	62.7	0.584	0.780	0.0019	0.0019	5.7	16.5	33.5	71.0
224	82.6	24.1	13.9	57.7	0.594	0.833	0.133	0.0024	8.6	22.5	38.6	28.4	0.0004	0.470	0.0085	62.7	0.584	0.818	0.0020	0.0020	7.3	17.7	34.8	79.3
225	66.6	24.1	13.9	57.7	0.594	0.833	0.133	0.0024	8.6	22.5	38.6	28.4	0.0004	0.470	0.0085	62.7	0.584	0.818	0.0020	0.0020	7.3	17.7	34.8	79.3
226	61.3	24.1	13.9	103.0	0.594	0.638	0.070	0.0033	3.6	17.5	34.9	28.4	0.0004	0.428	0.0199	112.1	0.584	0.607	0.0021	0.0021	2.3	13.7	30.3	68.0
227	77.5	24.1	13.9	103.0	0.594	0.701	0.077	0.0036	4.8	18.7	35.8	28.4	0.0004	0.428	0.0199	112.1	0.584	0.675	0.0024	0.0024	3.1	14.3	30.9	65.1
228	77.3	24.1	13.9	103.0	0.594	0.701	0.077	0.0036	4.8	18.7	35.8	28.4	0.0004	0.428	0.0199	112.1	0.584	0.675	0.0024	0.0024	3.1	14.3	30.9	65.1
229	55.0	24.1	13.9	31.3	0.594	0.890	0.347	0.0014	11.8	25.7	40.9	28.4	0.0004	0.342	0.0014	34.0	0.584	0.881	0.0012	0.0012	10.1	20.0	37.1	54.9
230	61.8	24.1	13.9	31.3	0.594	0.909	0.355	0.0014	14.6	28.5	42.9	28.4	0.0004	0.342	0.0014	34.0	0.584	0.901	0.0012	0.0012	12.5	21.9	39.0	68.1
231	70.3	24.1	13.9	31.3	0.594	0.909	0.355	0.0014	14.6	28.5	42.9	28.4	0.0004	0.342	0.0014	34.0	0.584	0.901	0.0012	0.0012	12.5	21.9	39.0	68.1
232	53.0	10.4	22.6	35.2	0.927	0.531	0.031	0.0015	15.0	37.6	38.9	12.2	0.0067	0.146	0.0068	38.3	0.912	0.489	0.0009	0.0009	9.4	25.2	32.5	55.8
233	55.0	10.4	22.6	35.2	0.927	0.765	0.045	0.0021	21.7	44.2	43.2	12.2	0.0067	0.146	0.0068	38.3	0.912	0.745	0.0014	0.0014	14.4	28.3	35.7	110.3
234	50.0	10.4	11.3	35.2	0.927	0.531	0.031	0.0015	20.0	31.3	32.9	12.2	0.0089	0.128	0.0060	38.3	0.912	0.489	0.0009	0.0009	12.6	17.6	25.0	43.6
235	52.0	10.4	11.3	35.2	0.927	0.765	0.045	0.0021	28.9	40.2	39.3	12.2	0.0089	0.128	0.0060	38.3	0.912	0.745	0.0014	0.0014	19.2	21.8	29.2	111.6
236	48.0	10.4	0.0	35.2	0.927	0.531	0.031	0.0015	40.1	40.1	37.8	12.2	0.0178	0.092	0.0043	38.3	0.912	0.489	0.0009	0.0009	25.2	16.1	23.4	46.5
237	55.0	10.4	0.0	35.2	0.927	0.765	0.045	0.0021	57.8	57.8	43.2	12.2	0.0178	0.092	0.0043	38.3	0.912	0.745	0.0014	0.0014	38.4	24.4	31.8	67.3
238	49.0	10.4	22.6	35.2	0.927	0.531	0.031	0.0015	30.0	52.6	43.2	12.2	0.0133	0.106	0.0049	38.3	0.912	0.489	0.0009	0.0009	18.9	31.2	36.7	78.6

No.	1	2	3	4	5	6	7	8	9	10	11	12	13	14	15	16	17	18	19	20	21	22	23	24
239	130.3	36.7	37.5	28.8	0.0014	0.0014	0.745	0.912	38.3	0.0049	0.106	0.0133	12.2	43.2	65.9	43.3	0.0021	0.045	0.765	0.927	35.2	22.6	10.4	50.0
240	170.9	57.0	24.4	38.2	0.0024	0.0026	0.752	1.032	62.0	0.0024	0.160	0.0257	54.4	83.9	61.8	61.8	0.0039	0.258	0.772	1.049	56.9	0.0	46.3	159.0
241	205.4	75.3	42.6	38.2	0.0024	0.0026	0.752	1.032	62.0	0.0024	0.160	0.0257	54.4	102.2	83.2	61.8	0.0039	0.258	0.772	1.049	56.9	21.4	46.3	205.6
242	222.0	105.5	72.7	45.0	0.0036	0.0036	0.717	1.032	70.8	0.0060	0.403	0.0011	54.4	112.3	93.5	50.6	0.0040	0.287	0.740	1.049	65.1	42.9	46.3	219.1
243	213.6	93.5	60.8	38.2	0.0024	0.0026	0.752	1.032	62.0	0.0024	0.160	0.0257	54.4	120.4	104.6	61.8	0.0039	0.258	0.772	1.049	56.9	42.9	46.3	225.6
244	234.4	86.3	53.6	27.0	0.0032	0.0032	0.643	1.032	89.2	0.0033	0.215	0.0300	54.4	100.3	76.9	34.0	0.0040	0.317	0.672	1.049	81.9	42.9	46.3	242.7
245	231.5	136.3	73.5	91.1	0.0040	0.0040	0.843	1.365	70.8	0.0065	0.438	0.0011	104.2	141.1	91.1	91.1	0.0040	0.439	0.855	1.387	65.1	0.0	88.6	213.6
246	268.3	127.7	65.1	45.5	0.0040	0.0040	0.843	1.365	70.8	0.0072	0.486	0.0008	104.2	136.5	78.9	45.5	0.0040	0.439	0.855	1.387	65.1	33.3	88.6	272.8
247	340.4	154.4	91.7	78.5	0.0027	0.0039	0.862	1.365	62.0	0.0027	0.182	0.0257	104.2	186.5	148.0	114.7	0.0040	0.387	0.873	1.387	56.9	33.3	88.6	297.5
248	327.8	137.4	74.7	57.4	0.0038	0.0052	0.802	1.365	89.2	0.0038	0.245	0.0300	104.2	147.8	94.5	61.2	0.0040	0.510	0.818	1.387	81.9	33.3	88.6	316.7
249	301.4	156.0	93.4	45.5	0.0040	0.0040	0.843	1.365	70.8	0.0072	0.486	0.0008	104.2	164.8	112.2	45.5	0.0040	0.439	0.855	1.387	65.1	66.6	88.6	309.8
250	97.9	42.7	15.4	19.0	0.0027	0.0027	0.529	1.101	67.2	0.0074	0.436	0.0009	45.4	49.9	23.6	23.6	0.0033	0.193	0.567	1.118	61.7	0.0	38.6	61.6
251	94.8	41.8	15.0	18.6	0.0026	0.0026	0.529	1.073	67.2	0.0073	0.432	0.0009	44.5	48.8	23.0	23.0	0.0032	0.189	0.567	1.090	61.7	0.0	37.9	59.7
252	92.6	47.0	20.9	25.9	0.0036	0.0036	0.764	1.035	67.2	0.0073	0.428	0.0009	43.4	52.1	28.7	28.7	0.0040	0.251	0.783	1.051	61.7	0.0	36.9	60.0
253	103.3	56.6	29.8	36.9	0.0037	0.0037	0.764	1.073	67.2	0.0067	0.393	0.0013	44.5	60.7	39.5	39.5	0.0040	0.261	0.783	1.090	61.7	0.0	37.9	80.7
254	93.9	47.5	20.6	25.6	0.0026	0.0026	0.529	1.075	67.2	0.0067	0.393	0.0013	44.6	55.2	31.7	31.7	0.0032	0.189	0.567	1.092	61.7	0.0	37.9	64.3
255	112.2	63.4	36.6	45.3	0.0037	0.0037	0.764	1.070	67.2	0.0063	0.369	0.0015	44.5	67.3	48.6	48.6	0.0040	0.260	0.783	1.087	61.7	0.0	37.8	90.0
256	168.2	89.0	45.1	25.9	0.0034	0.0034	0.815	1.096	55.6	0.0065	0.489	0.0007	73.0	99.0	59.0	30.5	0.0040	0.298	0.830	1.114	51.1	28.5	62.0	124.4
257	168.2	89.0	45.1	25.9	0.0034	0.0034	0.815	1.096	55.6	0.0065	0.489	0.0007	73.0	99.0	59.0	30.5	0.0040	0.298	0.830	1.114	51.1	28.5	62.0	130.0
258	204.9	115.6	71.7	58.8	0.0024	0.0024	0.876	1.096	37.2	0.0046	0.346	0.0021	73.0	126.6	97.3	68.8	0.0028	0.213	0.886	1.114	34.2	28.5	62.0	148.0
259	279.7	194.2	117.6	145.6	0.0040	0.0040	0.720	1.817	70.1	0.0088	0.461	0.0012	127.1	197.0	145.6	145.6	0.0040	0.390	0.742	1.846	64.4	0.0	108.0	306.1
260	279.5	151.3	74.8	92.6	0.0040	0.0040	0.635	1.817	91.1	0.0100	0.528	0.0008	127.1	158.8	92.6	92.6	0.0040	0.455	0.665	1.846	83.8	0.0	108.0	246.7
261	284.4	196.4	117.6	145.6	0.0040	0.0040	0.720	1.888	70.1	0.0089	0.467	0.0012	130.8	199.7	145.6	145.6	0.0040	0.406	0.742	1.919	64.4	0.0	111.2	257.2
262	263.0	154.6	83.1	103.0	0.0040	0.0040	0.720	1.656	70.1	0.0085	0.449	0.0012	118.6	160.1	103.0	103.0	0.0040	0.356	0.742	1.683	64.4	0.0	100.8	260.6
263	284.3	255.4	176.3	218.4	0.0040	0.0040	0.778	1.888	55.4	0.0079	0.413	0.0018	130.8	252.3	218.4	218.4	0.0040	0.344	0.796	1.919	50.9	0.0	111.2	334.3
264	96.7	48.2	17.2	21.3	0.0021	0.0021	0.909	1.229	27.4	0.0035	0.439	0.0006	51.5	55.2	24.9	24.9	0.0024	0.302	0.916	1.248	25.2	0.0	43.8	61.0
265	110.2	65.3	34.4	42.6	0.0021	0.0021	0.909	1.229	27.4	0.0029	0.356	0.0012	51.3	73.0	49.7	49.7	0.0024	0.302	0.916	1.248	25.2	0.0	43.6	89.8
266	67.5	38.6	22.1	27.4	0.0022	0.0022	0.817	1.477	27.4	0.0029	0.358	0.0014	27.4	43.1	32.3	32.3	0.0026	0.330	0.832	1.501	25.2	0.0	23.3	55.6
267	52.0	60.7	44.2	54.8	0.0022	0.0022	0.817	1.477	27.4	0.0023	0.291	0.0028	27.2	66.3	64.5	64.5	0.0026	0.330	0.832	1.501	25.2	0.0	23.1	71.5
268	63.3	21.2	5.2	6.4	0.0034	0.0110	0.860	1.283	186.0	0.0034	0.369	0.0072	28.5	26.1	7.7	7.7	0.0040	0.750	0.709	1.303	170.9	0.0	24.2	66.0
269	67.3	22.2	6.5	8.0	0.0021	0.0021	0.244	1.283	124.4	0.0024	0.266	0.0144	28.5	25.6	6.9	6.9	0.0018	0.197	0.144	1.303	114.4	0.0	24.2	69.0
270	78.9	17.5	0.5	0.6	0.0001	0.0001	0.017	1.283	98.3	0.0020	0.220	0.0216	28.5	24.5	5.5	5.5	0.0010	0.104	0.096	1.303	90.4	0.0	24.2	75.0
271	85.0	30.4	14.3	6.5	0.0034	0.0111	0.860	1.295	186.0	0.0034	0.370	0.0072	28.7	35.4	18.3	7.7	0.0040	0.750	0.709	1.316	170.9	10.7	24.4	88.0
272	87.9	31.4	15.6	8.1	0.0021	0.0021	0.244	1.295	124.4	0.0024	0.267	0.0144	28.7	34.8	17.6	7.0	0.0018	0.199	0.144	1.316	114.4	10.7	24.4	90.0
273	95.4	26.7	9.6	0.6	0.0001	0.0001	0.017	1.295	98.3	0.0020	0.221	0.0216	28.7	33.8	16.2	5.5	0.0010	0.105	0.096	1.316	90.4	10.7	24.4	91.0
274	96.3	35.0	18.9	6.5	0.0034	0.0111	0.860	1.295	186.0	0.0034	0.370	0.0072	28.7	39.9	23.7	7.7	0.0040	0.750	0.709	1.316	170.9	16.0	24.4	90.0
275	98.9	36.0	20.1	8.1	0.0021	0.0021	0.244	1.295	124.4	0.0024	0.267	0.0144	28.7	39.4	23.0	7.0	0.0018	0.199	0.144	1.316	114.4	16.0	24.4	93.0
276	106.1	31.3	14.2	0.6	0.0001	0.0001	0.017	1.295	98.3	0.0020	0.221	0.0216	28.7	38.3	21.5	5.5	0.0010	0.105	0.096	1.316	90.4	16.0	24.4	98.0
277	54.1	26.1	18.8	8.9	0.0029	0.0029	0.611	0.994	69.9	0.0074	0.411	0.0010	12.2	28.2	24.5	10.9	0.0035	0.195	0.643	1.010	64.3	13.6	10.3	65.0
278	54.1	26.1	18.8	8.9	0.0029	0.0029	0.611	0.994	69.9	0.0074	0.411	0.0010	12.2	28.2	24.5	10.9	0.0035	0.195	0.643	1.010	64.3	13.6	10.3	45.9
279	89.9	28.9	21.6	12.4	0.0040	0.0040	///	///	///	///	///	///	12.2	30.4	26.0	12.4	0.0040	///	///	///	///	13.6	10.3	66.1
280	89.9	28.9	21.6	12.4	0.0040	0.0040	///	///	///	///	///	///	12.2	30.4	26.0	12.4	0.0040	///	///	///	///	13.6	10.3	66.7

No.	$V_{U\text{-}exp}$	V_c	V_s	L_e	K_1	K_2	K_v	ε_{fe}	V_f	Check Equation (17)	$\emptyset V_{n\text{-}ACI}$	V_c	ρ_{frp}	R	$\varepsilon_{frpe\text{-}1}$	L_e	K_1	K_2	$\varepsilon_{frpe\text{-}2}$	Min. ε_{frpe}	V_{frp}	Check Equation (30)	$V_{r\text{-}ABA}$	V_{ANN}
281	154.6	40.7	53.7	43.0	1.010	0.881	0.179	0.0032	39.9	93.5	109.0	47.9	0.0010	0.411	0.0074	46.8	0.994	0.870	0.0027	0.0027	34.0	73.1	101.9	168.0
282	159.8	40.7	53.7	43.0	1.010	0.881	0.179	0.0032	39.9	93.5	109.0	47.9	0.0010	0.411	0.0074	46.8	0.994	0.870	0.0027	0.0027	34.0	73.1	101.9	168.0
283	236.4	40.7	53.7	///	///	///	///	0.0040	49.6	103.3	120.3	47.9	///	///	///	///	///	///	0.0040	0.0040	49.6	85.7	114.6	230.0
284	250.3	40.7	53.7	///	///	///	///	0.0040	49.6	103.3	120.3	47.9	///	///	///	///	///	///	0.0040	0.0040	49.6	85.7	114.6	230.0
285	563.4	176.2	232.2	28.8	1.010	0.960	0.130	0.0023	116.3	348.6	431.2	207.3	0.0010	0.411	0.0074	31.3	0.994	0.957	0.0020	0.0020	100.2	278.3	402.9	560.7
286	559.8	176.2	232.2	28.8	1.010	0.960	0.130	0.0023	116.3	348.6	431.2	207.3	0.0010	0.411	0.0074	31.3	0.994	0.957	0.0020	0.0020	100.2	278.3	402.9	560.7
287	871.6	176.2	232.2	///	///	///	///	0.0040	198.5	430.8	507.5	207.3	///	///	///	///	///	///	0.0040	0.0040	198.5	357.7	482.6	876.6
288	881.2	176.2	232.2	///	///	///	///	0.0040	198.5	430.8	507.5	207.3	///	///	///	///	///	///	0.0040	0.0040	198.5	357.7	482.6	876.6
289	102.4	45.2	0.0	92.3	0.950	0.675	0.355	0.0040	31.5	31.5	61.2	53.2	0.0008	0.433	0.0061	100.4	0.935	0.646	0.0040	0.0040	31.5	25.4	57.4	121.2
290	120.0	45.2	0.0	66.0	0.950	0.768	0.289	0.0040	56.2	56.2	79.0	53.2	0.0014	0.364	0.0051	71.8	0.935	0.747	0.0034	0.0034	47.7	38.6	70.6	123.3
291	121.7	45.2	0.0	44.1	0.950	0.845	0.213	0.0030	83.5	83.5	98.8	53.2	0.0028	0.295	0.0041	48.0	0.935	0.831	0.0025	0.0025	71.0	57.4	89.5	128.3
292	282.0	45.2	84.4	92.3	0.950	0.675	0.355	0.0040	31.5	115.9	133.0	53.2	0.0008	0.433	0.0061	100.4	0.935	0.646	0.0040	0.0040	31.5	97.2	129.2	274.2
293	255.0	45.2	84.4	66.0	0.950	0.768	0.289	0.0040	56.2	140.6	150.8	53.2	0.0014	0.364	0.0051	71.8	0.935	0.747	0.0034	0.0034	47.7	110.3	142.4	275.6
294	267.2	45.2	84.4	44.1	0.950	0.845	0.213	0.0030	83.5	168.0	170.6	53.2	0.0028	0.295	0.0041	48.0	0.935	0.831	0.0025	0.0025	71.0	129.1	159.6	278.9
295	309.4	45.2	168.9	66.0	0.950	0.768	0.289	0.0040	56.2	225.0	187.7	53.2	0.0014	0.364	0.0051	71.8	0.935	0.747	0.0034	0.0034	47.7	182.1	159.6	286.5
296	297.2	45.2	168.9	44.1	0.950	0.845	0.213	0.0030	83.5	252.4	187.7	53.2	0.0028	0.295	0.0041	48.0	0.935	0.831	0.0025	0.0025	71.0	200.9	159.6	288.7
297	207.0	85.7	77.7	///	///	///	///	0.0040	66.7	144.4	192.7	100.8	///	///	///	///	///	///	0.0040	0.0040	66.7	119.9	180.6	217.0
298	154.0	55.1	0.0	57.2	1.183	0.542	0.162	0.0031	48.7	48.7	82.0	64.8	0.0016	0.419	0.0080	62.3	1.164	0.502	0.0025	0.0025	39.0	31.5	70.5	132.7
299	94.5	55.1	0.0	57.2	1.183	0.542	0.162	0.0031	24.4	24.4	64.4	64.8	0.0008	0.516	0.0098	62.3	1.164	0.502	0.0025	0.0025	19.5	15.7	54.7	129.0
300	108.0	55.1	0.0	45.5	1.183	0.636	0.192	0.0029	67.6	67.6	95.6	64.8	0.0016	0.372	0.0056	49.4	1.164	0.604	0.0024	0.0024	55.5	44.8	83.8	137.8
301	110.0	55.1	0.0	45.5	1.183	0.636	0.192	0.0029	95.6	95.6	115.9	64.8	0.0016	0.372	0.0056	49.4	1.164	0.604	0.0024	0.0024	78.4	63.3	102.4	137.8
302	137.0	68.1	44.8	22.6	1.334	0.823	0.099	0.0021	166.8	211.6	216.5	80.1	0.0071	0.278	0.0058	24.6	1.313	0.807	0.0018	0.0018	141.5	50.1	200.7	135.0
303	141.0	68.1	44.8	22.6	1.334	0.823	0.099	0.0021	166.8	211.6	216.5	80.1	0.0071	0.278	0.0058	24.6	1.313	0.807	0.0018	0.0018	141.5	124.4	200.7	135.0
304	146.0	68.1	44.8	52.4	1.334	0.813	0.398	0.0040	116.7	161.5	180.2	80.1	0.0009	0.429	0.0051	57.0	1.313	0.797	0.0040	0.0040	116.7	42.7	180.6	158.5

The cells marked in green indicate the positives of the conditional statement and the cells marked in pink indicate the negatives of the conditional statement.

Reference

Abdel-Jaber, M. S., Walker, P. R., & Hutchinson, A. R. (2003). Shear strengthening of reinforced concrete beams using different configurations of externally bonded carbon fibre reinforced plates. *Materials and Structures*, *36*, 291–301. https://doi.org/10.1007/BF02480868.

Adhikary, B. B., & Mutsuyoshi, H. (2004). Behavior of concrete beams strengthened in shear with carbon-fiber sheets. *Journal of Composites for Construction*, *8*(3), 258–264. https://doi.org/10.1061/(ASCE)1090-0268(2004)8:3(258).

Al-Sulaimani, G. J., Sharif, A., Basunbul, I. A., Baluch, M. H., & Ghaleb, B. N. (1994). Shear repair for reinforced concrete by fiberglass plate bonding. *Structural Journal*, *91*(4), 458–464. https://doi.org/10.14359/4153.

Alambeigi, K., Mohammadimehr, M., Bamdad, M., & Rabczuk, T. (2020). Free and forced vibration analysis of a sandwich beam considering porous core and SMA hybrid composite face layers on Vlasov's foundation. *Acta Mechanica*, *231*, 3199–3218. https://doi.org/10.1007/s00707-020-02697-5.

Alwosheel, A., Cranenburgh, S. van, & Chorus, C. G. (2018). Is your dataset big enough? Sample size requirements when using artificial neural networks for discrete choice analysis. *Journal of Choice Modelling*, *28*, 167–182. https://doi.org/10.1016/j.jocm.2018.07.002.

Alzate, A., Arteaga, A., Diego, A. de, Cisneros, D., & Perera, R. (2013). Shear strengthening of reinforced concrete members with CFRP sheets. *Materiales de Construcción*, *63*(310), 251–265. https://doi.org/10.3989/mc.2012.06611.

American Concrete Institute (ACI) (1996). *440R-96: State-of-the-Art Report on Fiber Reinforced Plastic (FRP) Reinforcement for Concrete Structures*. https://www.concrete.org/store/productdetail.aspx?ItemID=44096.

American Concrete Institute (ACI) (2005). *318M-05: Building Code Requirements for Structural Concrete and Commentary*. https://www.concrete.org/?TabID=411&ItemID=31805.

American Concrete Institute (ACI) (2008). *440.2R-08: Guide for the Design and Construction of Externally Bonded FRP Systems for Strengthening Concrete Structures*. https://www.concrete.org/store/productdetail.aspx?ItemID=440208.

Areias, P., Pires, M., Bac, N. V., & Rabczuk, T. (2019). An objective and path-independent 3D finite-strain beam with least-squares assumed-strain formulation. *Computational Mechanics*, *64*, 1115–1131. https://doi.org/10.1007/s00466-019-01696-1.

Barros, J. A. O., & Dias, S. J. E. (2006). Near surface mounted CFRP laminates for shear strengthening of concrete beams. *Cement and Concrete Composites*, *28*(3), 276–292. https://doi.org/10.1016/j.cemconcomp.2005.11.003.

Beber, A., & Campos Filho, A. (2005). CFRP composites on the shear strengthening of reinforced concrete beams. *Revista IBRACON de Estruturas e Materiais*, *1*(3), 127–143.

Bousselham, A., & Chaallal, O. (2006). Effect of transverse steel and shear span on the performance of RC beams strengthened in shear with CFRP. *Composites Part B: Engineering*, *37*(1), 37–46. https://doi.org/10.1016/j.compositesb.2005.05.012.

Bukhari, I. A., Vollum, R. L., Ahmad, S., & Sagaseta, J. (2010). Shear strengthening of reinforced concrete beams with CFRP. *Magazine of Concrete Research*, *62*(1), 65–77. https://doi.org/10.1680/macr.2008.62.1.65.

Bukhari, I. A., Vollum, R., Ahmad, S., & Sagaseta, J. (2013). Shear strengthening of short span reinforced concrete beams with CFRP sheets. *Arabian Journal for Science and Engineering*, *38*, 523–536. https://doi.org/10.1007/s13369-012-0333-z.

Canadian Standard Association (CSA) (2002). *Design and Construction of Building Components with Fiber-Reinforced Polymers* (CAN/CSA-S806-02 (R2007)). CSA Group.

Cao, S. Y., Chen, J. F., Teng, J. G., Hao, Z., & Chen, J. (2005). Debonding in RC beams shear strengthened with complete FRP wraps. *Journal of composites for construction*, *9*(5), 417–428. https://doi.org/10.1061/(ASCE)1090-0268(2005)9:5(417).

Carolin, A., & Täljsten, B. (2005). Experimental study of strengthening for increased shear bearing capacity. *Journal of Composites for Construction*, *9*(6), 488–496. https://doi.org/10.1061/(ASCE)1090-0268(2005)9:6(488).

Chaallal, O., Nollet, M. J., & Perraton, D. (1988). Shear strengthening of RC beams by externally bonded side CFRP strips. *Journal of Composites for Construction*, *2*(2), 111–113. https://doi.org/10.1061/(ASCE)1090-0268(1998)2:2(111).

Chen, J. F., & Teng, J. G. (2003). Shear capacity of FRP-strengthened RC beams: FRP debonding. *Construction and Building Materials*, *17*(1), 27–41. https://doi.org/10.1016/S0950-0618(02)00091-0.

Collins, F., & Roper, H. (1990). Laboratory investigation of shear repair of reinforced concrete beams loaded in flexure. *Materials Journal*, *87*(2), 149–159.

Dadgar-Rad, F., & Firouzi, N. (2021). Large deformation analysis of two-dimensional visco-hyperelastic beams and frames. *Archive of Applied Mechanics*, *91*, 4279–4301. https://doi.org/10.1007/s00419-021-02008-x.

Deniaud, C., & Cheng, J. J. R. (2001). Review of shear design methods for reinforced concrete beams strengthened with fiber reinforced polymer sheets. *Canadian Journal of Civil Engineering*, *28*(2), 271–281. https://doi.org/10.1139/l00-113.

Diagana, C., Li, A., Gedalia, B., & Delmas, Y. (2003). Shear strengthening effectiveness with CFF strips. *Engineering Structures*, *25*(4), 507–516. https://doi.org/10.1016/S0141-0296(02)00208-0.

Dias, S. J. E., & Barros, J. A. O. (2012). Experimental behaviour of RC beams shear strengthened with NSM CFRP laminates. *Strain*, *48*(1), 88–100. https://doi.org/10.1111/j.1475-1305.2010.00801.x.

Firouzi, N., & Kazemi, S. R. (2023). Investigation on dynamic stability of Timoshenko beam using axial parametric excitation. *Applied Physics A*, *129*(12), 869. https://doi.org/10.1007/s00339-023-07155-2.

Gamino, A. L., Sousa, J. L. A. O., Manzoli, O. L., & Bittencourt, T. N. (2010). R/C structures strengthened with CFRP. Part II: analysis of shear models. *Revista IBRACON de Estruturas e Materiais*, *3*, 24–49. https://doi.org/10.1590/S1983-41952010000100003.

Grace, N. F., Ragheb, W. F., & Abdel-Sayed, G. (2003). Flexural and shear strengthening of concrete beams using new triaxially braided ductile fabric. *Structural Journal*, *100*(6), 804–814. https://doi.org/10.14359/12847

Grande, E., Imbimbo, M., & Rasulo, A. (2009). Effect of transverse steel on the response of RC beams strengthened in shear by FRP: Experimental study. *Journal of Composites for Construction*, *13*(5), 405–414. https://doi.org/10.1061/(ASCE)1090-0268(2009)13:5(405).

Ianniruberto, U., & Imbimbo, M. (2004). Role of fiber reinforced plastic sheets in shear response of reinforced concrete beams: Experimental and analytical results. *Journal of Composites for Construction*, *8*(5), 415–424. https://doi.org/10.1061/(ASCE)1090-0268(2004)8:5(415).

International Federation for Structural Concrete (fib) (2001). *Externally bonded FRP reinforcement for RC structures*. https://doi.org/10.35789/fib.BULL.0014.

Islam, M. R., Mansur, M. A., & Maalej, M. (2005). Shear strengthening of RC deep beams using externally bonded FRP systems. *Cement and Concrete Composites*, *27*(3), 413–420. https://doi.org/10.1016/j.cemconcomp.2004.04.002.

Kamiharako, A., Maruyama, K., Takada, K., & Shimomura, T. (1997). Evaluation of shear contribution of FRP sheets attached to concrete beams. In *Non-Metallic (FRP) Reinforcement for Concrete Structures. Proceedings of the Third International Symposium (FRPRCS-3). Sapporo, Japan 14–16 October 1997* (Vol. 1, pp. 467–474). Japan Concrete Institute.

Karami, B., Janghorban, M., & Rabczuk, T. (2020). Dynamics of two-dimensional functionally graded tapered Timoshenko nanobeam in thermal environment using nonlocal strain gradient theory. *Composites Part B: Engineering*, *182*, 107622. https://doi.org/10.1016/j.compositesb.2019.107622.

Kasabov, N. K. (1996). *Foundations of Neural Networks, Fuzzy Systems, and Knowledge Engineering*. MIT Press. https://doi.org/10.7551/mitpress/3071.001.0001.

Khalifa, A., & Nanni, A. (2000). Improving shear capacity of existing RC T-section beams using CFRP composites. *Cement and Concrete Composites*, *22*(3), 165–174. https://doi.org/10.1016/S0958-9465(99)00051-7.

Khalifa, A., & Nanni, A. (2002). Rehabilitation of rectangular simply supported RC beams with shear deficiencies using CFRP composites. *Construction and building materials*, *16*(3), 135–146. https://doi.org/10.1016/S0950-0618(02)00002-8.

Khalifa, A., Tumialan, G., Nanni, A., & Belarbi, A. (1999). Shear strengthening of continuous reinforced concrete beams using externally bonded carbon fiber reinforced polymer sheets. *Scientific Programming*, *188*, 995–1008.

Kim, G., Sim, J., & Oh, H. (2008). Shear strength of strengthened RC beams with FRPs in shear. *Construction and Building Materials*, *22*(6), 1261–1270. https://doi.org/10.1016/j.conbuildmat.2007.01.021.

Leung, C. K., Chen, Z., Lee, S., Ng, M., Xu, M., & Tang, J. (2007). Effect of size on the failure of geometrically similar concrete beams strengthened in shear with FRP strips. *Journal of Composites for Construction*, *11*(5), 487–496. https://doi.org/10.1061/(ASCE)1090-0268(2007)11:5(487).

Mabsout, M., Tarhini, K., Jabakhanji, R., & Awwad, E. (2004). Wheel load distribution in simply supported concrete slab bridges. *Journal of Bridge Engineering*, *9*(2), 147–155. https://doi.org/10.1061/(ASCE)1084-0702(2004)9:2(147).

Management and Planning Organization of Iran (MPO) (2006). *The guideline for design specification of strengthening RC buildings using fiber reinforced polymers (FRP)* (Publication No. 345). Office of Technical Affairs Deputy Technical, Criteria Codification and Earthquake Risk Reduction Affairs Bureau.

Maruyama, K. (Ed.) (2001). *I. Recommendations for upgrading of concrete structures with use of continuous fiber sheet*. Japan Society of Civil Engineers.

Mirmiran, A., Shahawy, M., Nanni, A., Karbhari, V. (2004). *Bonded Repair and Retrofit of Concrete Structures Using FRP Composites – Recommended Construction Specifications and Process Control Manual* (NCHRP Report 514). Transportation Research Board. https://doi.org/10.17226/22034.

Mofidi, A., & Chaallal, O. (2014). Tests and design provisions for reinforced-concrete beams strengthened in shear using FRP sheets and strips. *International Journal of Concrete Structures and Materials*, *8*, 117–128. https://doi.org/10.1007/s40069-013-0060-1.

Mofidi, A., Thivierge, S., Chaallal, O., & Shao, Y. (2014). Behavior of reinforced concrete beams strengthened in shear using L-shaped CFRP plates: Experimental investigation. *Journal of Composites for Construction*, *18*(2), 04013033. https://doi.org/10.1061/(ASCE)CC.1943-5614.0000398.

Monti, G., & Liotta, M. A. (2007). Tests and design equations for FRP-strengthening in shear. *Construction and Building Materials*, *21*(4), 799–809. https://doi.org/10.1016/j.conbuildmat.2006.06.023.

Noël, M., & Soudki, K. (2011). Evaluation of FRP posttensioned slab bridge strips using AASHTO-LRFD bridge design specifications. *Journal of Bridge Engineering*, *16*(6), 839–846. https://doi.org/10.1061/(ASCE)BE.1943-5592.0000226.

Norris, T., Saadatmanesh, H., & Ehsani, M. R. (1997). Shear and flexural strengthening of R/C beams with carbon fiber sheets. *Journal of Structural Engineering*, *123*(7), 903–911. https://doi.org/10.1061/(ASCE)0733-9445(1997)123:7(903).

Ozden, S., Atalay, H. M., Akpinar, E., Erdogan, H., & Vulaş, Y. Z. (2014). Shear strengthening of reinforced concrete T-beams with fully or partially bonded fibre-reinforced polymer composites. *Structural Concrete*, *15*(2), 229–239. https://doi.org/10.1002/suco.201300031.

Panda, K. C., Bhattacharyya, S. K., & Barai, S. V. (2011). Shear strengthening of RC T-beams with externally side bonded GFRP sheet. *Journal of Reinforced Plastics and Composites*, *30*(13), 1139–1154. https://doi.org/10.1177/0731684411417202.

Pellegrino, C., & Modena, C. (2002). Fiber reinforced polymer shear strengthening of reinforced concrete beams with transverse steel reinforcement. *Journal of Composites for Construction*, *6*(2), 104–111. https://doi.org/10.1061/(ASCE)1090-0268(2002)6:2(104).

Pellegrino, C., & Modena, C. (2008). An experimentally based analytical model for the shear capacity of FRP-strengthened reinforced concrete beams. *Mechanics of Composite Materials*, *44*, 231–244. https://doi.org/10.1007/s11029-008-9016-y.

Saadatmanesh, H., & Ehsani, M. R. (1991). RC beams strengthened with GFRP plates. I: Experimental study. *Journal of Structural Engineering*, *117*(11), 3417–3433. https://doi.org/10.1061/(ASCE)0733-9445(1991)117:11(3417).

Shahawy, M. A., Arockiasamy, M., Beitelman, T., & Sowrirajan, R. (1996). Reinforced concrete rectangular beams strengthened with CFRP laminates. *Composites Part B: Engineering*, *27*(3–4), 225–233. https://doi.org/10.1016/1359-8368(95)00044-5.

Singh, S. B. (2013). Shear response and design of RC beams strengthened using CFRP laminates. *International Journal of Advanced Structural Engineering*, *5*, 1–16. https://doi.org/10.1186/2008-6695-5-16.

Sobuz, H. R., Ahmed, E., Hasan, N. M. S., & Uddin, A. (2011). Use of carbon fiber laminates for strengthening reinforced concrete beams in bending. *International Journal of Civil & Structural Engineering*, *2*(1), 67–84.

Sundarraja, M. C., & Rajamohan, S. (2009). Strengthening of RC beams in shear using GFRP inclined strips – An experimental study. *Construction and Building Materials*, *23*(2), 856–864. https://doi.org/10.1016/j.conbuildmat.2008.04.008.

Tanarslan, H. M., Ertutar, Y., & Altin, S. (2008). The effects of CFRP strips for improving shear capacity of RC beams. *Journal of Reinforced Plastics and Composites*, *27*(12), 1287–1308. https://doi.org/10.1177/0731684407087370.

Täljsten, B. (2003). Strengthening concrete beams for shear with CFRP sheets. *Construction and Building Materials*, *17*(1), 15–26. https://doi.org/10.1016/S0950-0618(02)00088-0.

Teng, J. G., Chen, G. M., Chen, J. F., Rosenboom, O. A., & Lam, L. (2009). Behavior of RC beams shear strengthened with bonded or unbonded FRP wraps. *Journal of Composites for Construction*, *13*(5), 394–404. https://doi.org/10.1061/(ASCE)CC.1943-5614.0000040.

Triantafillou, T. C., & Antonopoulos, C. P. (2000). Design of concrete flexural members strengthened in shear with FRP. *Journal of Composites for Construction*, *4*(4), 198–205. https://doi.org/10.1061/(ASCE)1090-0268(2000)4:4(198).

Triantafillou, T. C., & Plevris, N. (1992). Strengthening of RC beams with epoxy-bonded fibre-composite materials. *Materials and Structures*, *25*, 201–211. https://doi.org/10.1007/BF02473064.

Umezu, K., Fujita, M., Nakai, H., & Tamaki, K. (1997). Shear behavior of RC beams with aramid fiber sheet. In *Non-Metallic (FRP) Reinforcement for Concrete Structures. Proceedings of the Third International Symposium (FRPRCS-3). Sapporo, Japan 14–16 October 1997* (Vol 1, pp. 491–498). Japan Concrete Institute.

Zhang, Z., & Hsu, Ch.-T. T. (2005). Shear strengthening of reinforced concrete beams using carbon-fiber-reinforced polymer laminates. *Journal of Composites for Construction*, *9*(2), 158–169. https://doi.org/10.1061/(ASCE)1090-0268(2005)9:2(158).

Zhang, Z., Hsu, Ch.-T. T., & Moren, J. (2004). Shear strengthening of reinforced concrete deep beams using carbon fiber reinforced polymer laminates. *Journal of Composites for Construction*, *8*(5), 403–414. https://doi.org/10.1061/(ASCE)1090-0268(2004)8:5(403).

Żur, K. K., Firouzi, N., Rabczuk, T., & Zhuang, X. (2023). Large deformation of hyperelastic modified Timoshenko–Ehrenfest beams under different types of loads. *Computer Methods in Applied Mechanics and Engineering*, *416*, 116368. https://doi.org/10.1016/j.cma.2023.116368.